Validation of a practice-oriented floor spectra formulation through actual data from the 2016/2017 Central Italy earthquake

Stefania Degli Abbati (stefania.degliabbati@unige.it)
University of Genoa: Universita degli Studi di Genova https://orcid.org/0000-0001-9991-8599
Serena Cattari
Università degli Studi di Genova: Universita degli Studi di Genova
Sergio Lagomarsino
Università degli Studi di Genova: Universita degli Studi di Genova

Research Article

Keywords: floor spectra, masonry, buildings permanently monitored, seismic analysis, non-structural elements

Posted Date: February 24th, 2022

DOI: https://doi.org/10.21203/rs.3.rs-1362727/v1

Validation of a practice-oriented floor spectra formulation through actual data from the 2016/2017 Central Italy earthquake

Stefania Degli Abbati[1*], Serena Cattari[1], Sergio Lagomarsino[1]

[1] DICCA, Dept. of Civil, Chemical Environmental Engineering, University of Genova Via Montallegro 1, Genova 16145, Italy

E-mail: stefania.degliabbati@unige.it, serena.cattari@unige.it, sergio.lagomarsino@unige.it

[*]Corresponding author

Abstract: Analytical expressions for the floor spectra evaluation play a key role for a correct definition of the seismic input induced to non-structural elements or local mechanisms in existing buildings. They have to be able to properly assess the possible amplification phenomena, but also to correctly describe the effects of nonlinearities due to structural damage. Due to the complexity of such phenomena, data on existing structures hit by earthquakes constitute a precious source for a better understanding of the topic and the validation of analytical expressions. In this framework, the paper aim is twofold. On one hand, it evaluates the entity of seismic amplification through experimental evidence from *in-situ* measurements on existing monitored structures. On the other hand, it presents the application of an analytical expression for the floor spectra already developed by the Authors to two unreinforced masonry (URM) buildings. The case-studies are the former Fabriano courthouse (Ancona, Italy) and the Pizzoli's town hall (L'Aquila, Italy). They were both hit by the 2016/2017 earthquake in Central Italy and are permanently monitored by the Italian seismic monitoring system of the Italian Department of Civil Protection (DPC). With the aim of the validation, the paper shows the comparison between experimental and analytical floor spectra for various minor events and mainshocks of the Central Italy earthquake. Since the two case-studies exhibited different damage level (from slight to moderate, respectively), the comparison allowed to verify the reliability of the expression both in the pseudo-elastic and moderate nonlinear fields.

Keywords: *floor spectra; masonry; buildings permanently monitored; seismic analysis; non-structural elements*

1 Introduction

In the seismic assessment of existing buildings, a crucial and tricky aspect is the proper definition of the seismic input to be used for the verification of acceleration-sensitive non-structural elements or local out-of-plane mechanisms in masonry buildings. Traditionally, the approach recommended by Codes (*e.g.* Eurocode 8, 2004; ASCE/SEI 7-10, 2010; New Zealand Code, 2017; Commentary of the Italian Technical Code, 2019) refers to the definition of the seismic action in terms of floor spectra that, as known, assume licit the decoupling between main and secondary structures (Chen and Soong, 1988; Muscolino, 1991).

The seismic input on an element housed at a certain level of a building is greatly influenced by the properties of both the primary structure and the element itself, that act as two filters connected in series. Due to this filtering effect, the characteristics of floor acceleration motions (*i.e.*, the induced motions at the base of the element) are markedly different from those of typical ground acceleration motions. The main parameters affecting the phenomenon are the characteristic of the ground motion (amplitude, frequency content and duration – Rodriguez et al., 2021), the dynamic response of the primary structure, the lateral load resisting system, the floor level and the level of nonlinearity of both primary structure and secondary element (Anajafi et al., 2019; Kazantzi et al., 2020a; Kazantzi et al., 2020b). Moreover, many additional parameters, such as diaphragm flexibility, torsional responses and also uncertainties in the inelastic behavior, can further amplify the seismic demands on secondary elements (Anajafi and Medina, 2019; Derakhshan et al., 2020). This research field is topical; thus, many numerical and experimental studies are available in literature, whose main findings are briefly summarized below.

Baggio et al. (2018) compare the ground with the floor acceleration time-histories computed in a Finite Element (FE) model of a complex masonry building (*i.e.* the Palazzo dei Musei in Modena, Italy). This comparison shows an important amplification phenomenon; moreover, the acceleration floor spectra numerically evaluated show that the host building acts as a filter, by amplifying the frequency content of the seismic input at the structural fundamental period. Analogous results were also experimentally observed in many shake-table campaigns (*e.g.* Senaldi et al., 2014; Magenes et al., 2014; Beyer et al., 2015; Senaldi et al., 2020). Furthermore, the results obtained by Baggio et. al. (2018) confirm that, in case of complex structures, the simplified expressions typically suggested by Codes for the evaluation of the fundamental period does not seem to be adequate.

A reduction in the acceleration amplification with an increasing nonlinear behavior is documented for unreinforced masonry (URM) buildings, *e.g.* in the numerical studies by Menon and Magenes (2011a) or in the experimental studies by Bothara et al. (2010) and Beyer et al. (2015). In the two latter works, the dynamic identification performed after each test highlighted that the fundamental frequencies gradually reduced when the prototype was exposed to excitations of increasing severity, while at the same time the structural damping increased; moreover, the transfer functions for the eaves level response acceleration computed by Bothara et al. (2010) shows a clear shift in frequency from a higher to a lower value during the shakings. This shift was ascribed by the authors to the decreasing of stiffness due to cracking but also due to inelastic rocking behavior of some piers in the prototype. Derakhshan et al. (2020) reviewed empirical data from nine buildings obtained from the Centre for Engineering Strong Motion Data (CESMD 2019) for a qualitative evaluation of the effects of diaphragm flexibility. The building height of the considered samples varied from 6.7 m to 12.6 m, while the horizontal diaphragms were made of timber sheathing on timber joists and/or steel framing. The acceleration amplification at the top of the walls (Amp_w) and at the mid-span of the diaphragms in short direction (Amp_d) was plotted as a function of the peak ground acceleration (PGA). The results showed an overall decrease in the amplification with an increase in earthquake intensity; a lack of correlation between amplifications and building height was instead found, mainly attributed by the authors to the diaphragm effects which have overshadowed the effect of building height on wall accelerations. Moreover, the large Amp_d/Amp_w ratio highlights the importance of considering diaphragm vibration effects when amplifying acceleration input to secondary components. Finally, the results of pushover and incremental dynamic analyses of equivalent frame (EF) models of four building typologies showed that the accelerations in buildings with flexible diaphragms are amplified by up to 3 when compared to the case of buildings with rigid diaphragms.

Another important parameter that can affect the floor spectra is the torsional response of the main building. For example, a study on instrumented buildings in California (USA) showed that the torsional responses of the supporting structure and/or the in-plane flexibility of floor diaphragms can increase by not negligible factors the seismic-induced force demands on elastic acceleration-sensitive non-structural components (Anajafi and Medina, 2019). Similarly, it is known that soil-structure interaction (SSI) can affect the acceleration response of the buildings (*e,g,* Karapetrou et al., 2015; Karatzetzou et al., 2015; de Silva et al., 2019; Fathi et al., 2020; Oz et al., 2020, Hamidia et al., 2021; Brunelli et al., 2021).

Available results of experimental tests are no doubt very useful to investigate the amplification phenomenon because they guarantee a detailed knowledge on both prototype and input. At the same time, numerical analyses on models allowed quantifying parametrically the effects on floor acceleration and floor spectra of many uncertainties, which are inherent in the characteristics of input ground excitation, primary structure and secondary elements themselves. However, experimental or numerical prototypes necessarily imply simplifications when compared to actual structures (due to lab or computational limitations, instrumentation needs, *etc.*). Thus, accurate data on existing structures hit by real seismic events are very valuable to understand the complexity of the phenomenon and to validate analytical expressions proposed in literature. The latter is a research field that gained increasing interest in the last years due to its important repercussion on the engineering practice (*e.g.* Menon and Magenes, 2011a-b; Sullivan et al., 2013; Calvi and Sullivan, 2014; Petrone et al., 2015; Vukobratović and Fajfar, 2016; Lucchini et al., 2017; Vukobratović and Fajfar, 2017; Surana et al., 2018; Degli Abbati et al., 2018; Merino et al., 2019; Di Domenico et al., 2021).

Within this context, the paper firstly describes the physics of the amplification phenomenon (§3) by means of the post-processing of some recordings on two unreinforced masonry (URM) buildings (§2), that are the former Fabriano courthouse (Ancona, Italy) and the Pizzoli's town hall (L'Aquila, Italy). They were selected within the aims of ReLUIS project founded by the Department of Civil Protection (DPC, Cattari et al., 2019), because they are permanently monitored by the Italian seismic monitoring network (Dolce et al., 2017), hereinafter briefly named as "OSS" (from the Italian name "*Osservatorio Sismico delle Strutture*"). The monitoring system includes accelerometers placed at the different levels plus a three-axial sensor at the foundation in order to measure the seismic excitation applied to the structure. Thus, records from different mainshocks, secondary seismic events and ambient noise are available as well.

Secondly, these data are used to validate the analytical expression proposed in 2018 by the Authors for the floor spectra definition (Degli Abbati et al., 2018). This expression allows evaluating the floor spectra in different points of the building and at different levels by considering the contribution of the more relevant modes, properly combined (§4). For the aim of the validation, the comparison of the experimental floor spectra (*i.e.* evaluated from the recorded accelerations) with the analytical ones is presented in the paper for the two above-mentioned case-studies (§5 and §6). Both were hit by the 2016/2017 Central Italy earthquake exhibiting from negligible to moderate damage levels, thus the comparison allowed validating the expression both in the pseudo-elastic field and for a slightly higher level of nonlinearity.

2 Dataset of monitored URM buildings hit by the Central Italy earthquake

The two examined case-studies are URM buildings built in the first half of '90s and characterized by external masonry façades with openings generally aligned and quite stiff diaphragms. Both are regular in elevation but with an irregular in plan configuration.

The former Fabriano courthouse (Fig. 1a) is a quite complex structure with four storeys (three completely above ground and one partially embedded) and a T-shaped plan; the total height is equal to 16.8 m and the average story area is equal to 1220 m^2. In 1999, after the Umbria and Marche earthquake (1997), the building was subjected to some strengthening interventions aimed to restore the damage and improve its seismic response. The most significant ones were: replacement of the original stairwell with a reinforced concrete (RC) one, disconnected from the main building through a seismic joint; strengthening interventions with reinforced plaster to vertical walls; local interventions of horizontal floors (sometimes replaced, sometimes reinforced with an additional RC slab); strengthening of the roof by means of a steel X-bracing; improvement of the wall-to-wall connections through reinforced riveting. The identification of the main structural interventions together with more data on geometry and constructive details are illustrated in Cattari et al. (2021).

Instead, the Pizzoli's town hall (Fig. 1b) presents a C-shaped floor plan, whose dimensions are about 38 x 12.5 m. It has two levels, a basement and a non-habitable attic characterized by a pavilion roof, composed of RC joists and hollow clay units and a 3 cm thick slab. The total height of the building is approximately 8.6 m. More details about geometry and constructive details can be found in Degli Abbati et al. (2021a).

Both case-studies were permanently instrumented by OSS as strategic buildings with a permanent accelerometric monitoring system. The latter is suitable for recording both strong-motion earthquakes and low vibrations and tremors, with accelerations from 10^{-4} to 2g. The sensor layout is shown in Fig. 1. Some accelerometers are bi-axial and were placed at different levels of the structure. One three-axial sensor was placed at the foundation level in order to measure the seismic input applied to the structure. The latter instrument is important to evaluate the amplification effects of the floor accelerations with respect to the ground/base excitation.

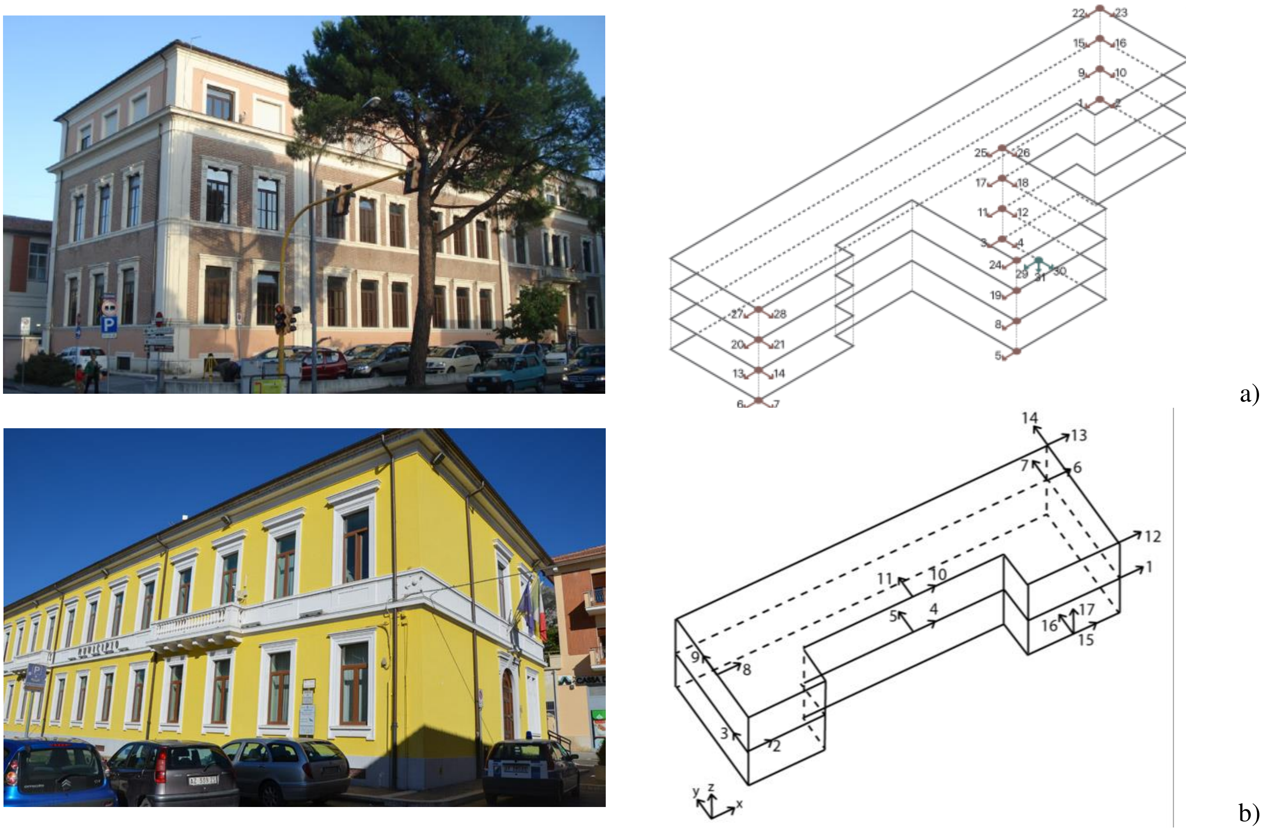

Fig. 1 Pictures and sensor location in the two examined case-studies: a) the former Fabriano courthouse; b) the Pizzoli's town hall.

The buildings were hit by the 2016/2017 Central Italy earthquake and exhibited very different levels of damage. A slight to negligible structural damage occurred on the Fabriano courthouse, while the Pizzoli's town hall was mostly hit by the mainshock of January 18, 2017 which induced the damage pattern sketched in Fig. 2.

Fig. 2 Damage survey detected on the Pizzoli's town hall during the *in-situ* inspections after the mainshock of 18/01/2017– figure adapted from Degli Abbati et al., 2021a.

Such damage was mainly concentrated in masonry piers at both levels and it was characterized by the presence of both pseudo-horizontal cracks (mainly associated with a flexural mode) and diagonal cracks (associated to a shear failure mechanism). In Fig. 2, the damage pattern detected on the building during an *in-situ* survey made by the ReLUIS research group (Cattari et al., 2019) was rated as follows: DL < DL2: negligible to low (cracks in grey); DL2<DL<DL3: moderate (cracks in red).

Starting from the data on geometry, constructive details and materials available from OSS, it was possible to set up a numerical model of each structure (Fig. 3a). The models were developed with the Tremuri software (Lagomarsino et al., 2013), that is based on the EF modelling approach, and calibrated and validated in previous studies (see Degli Abbati et al., 2021a for the Pizzoli's town hall and Cattari et al., 2021 for the former Fabriano courthouse). The EF approach considers only the in-plane behavior of masonry walls and concentrates the deformability and the nonlinear behavior into specific portions of URM walls, namely piers (vertical elements) and spandrels (masonry beams that connect piers). The approach can be considered reliable when the box behavior is guaranteed. This assumption is licit for both the case-studies, as demonstrated by the exhibited post-earthquake damage and deduced from the analysis of the constructive details.

The numerical models were calibrated in the elastic field using as target some dynamic identifications available in literature and performed with the ambient vibration data acquired by the OSS accelerometers, with a sampling frequency of 250 Hz. In particular:

- for the Fabriano courthouse, the target of the calibration process was the dynamic identification performed under operational conditions with the SSI-Cov algorithm and using the ambient noise of December 7, 2016 (Cattari et al., 2021);
- for the Pizzoli's town hall, the target was the dynamic identification provided by Sivori et al. (2021) performed using the ambient vibration data acquired on October 1, 2016 for one hour and employing the frequency domain decomposition technique with a frequency resolution of 0.05 Hz (Degli Abbati et al., 2021a).

The results of the elastic calibration of the numerical models are illustrated in Fig. 3b and c where a comparison between the measured (labeled "experimental") and numerical data (labeled "numerical") is reported in terms of frequencies (Fig. 3b) and MAC indexes (Fig. 3c - Allemange and Brown, 1982), respectively. The frequencies errors are expressed in percentage and reported in brackets on the X-axis of the histograms of Fig. 3b. After the model calibration, nonlinear dynamic analyses were performed through both models, using as input the accelerograms recorded by the sensors placed at the base of the buildings. The comparison between simulated and recorded response performed at global and local scales (*e.g.* in terms of hysteretic shear-displacement curves, damage pattern, accelerations on sensors and floor spectra) allowed also the models validation in the nonlinear range. For further details on model calibration and validation, interested readers may refer to Cattari et al. (2021) and Degli Abbati et al. (2021a). In the following, these models are used to assess the parameters useful to apply the analytical expression adopted for the computation of floor spectra.

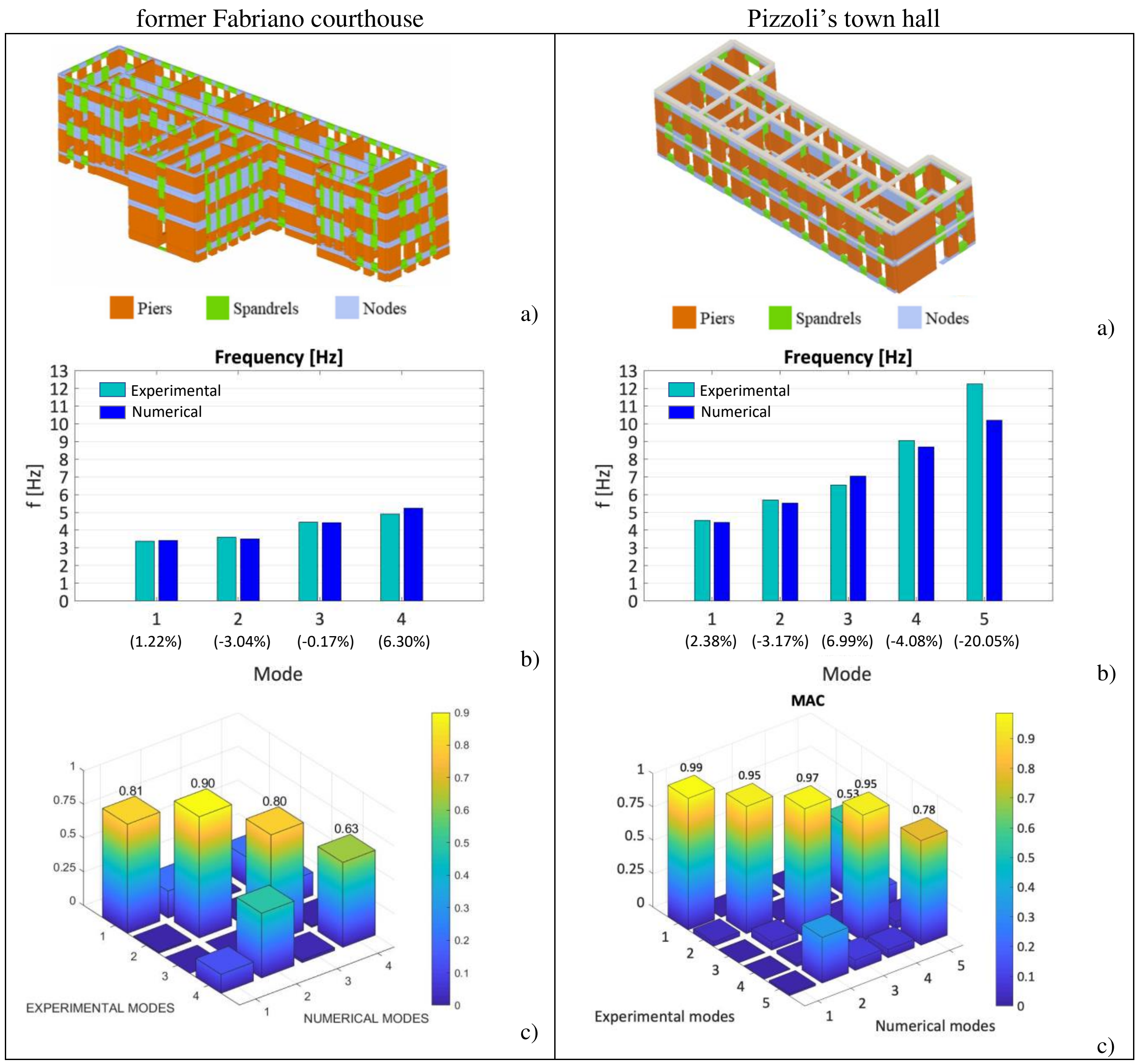

Fig. 3 For the two case-studies: a) Calibrated EF models; b) Comparison between measured and numerical frequencies (errors expressed on the X-axis in brackets); c) Comparison in terms of MAC indexes.

3 Physical interpretation of the amplification phenomenon for the investigated structures

Fig. 4 shows some post-processing of the recordings acquired by the permanent monitoring system on the two buildings presented in §2. In particular, Fig. 4a) compares, for the Fabriano courthouse and the Pizzoli's town hall, the response spectrum recorded at the base (dotted plot) with the floor spectra obtained from some sensors placed along the same vertical alignment, but at increasing height (thicker plot lines). In particular, the numbers of sensors are: 30, 10, 16 and 23 in the Y direction for the former Fabriano courthouse (sensor layout in Fig. 1a); 15, 1 and 12 in the X direction for the Pizzoli's town hall (sensor layout in Fig. 1b). The recordings refer to the two main events which mainly hit the structures during the Central Italy earthquake, *i.e.*: the second shake of the main event of 26/10/2016, for the Fabriano courthouse, and the mainshock of 18/01/2017, for the Pizzoli's town hall. This comparison clearly highlights the amplification phenomenon, which is in both cases more pronounced at the top and in correspondence of the fundamental periods in the direction of interest, that are: $T_{1,Y}$= 0.424 s, for the former Fabriano courthouse (this corresponds to mode 1 in Fig. 5, that is the main period in the Y direction); $T_{1,X}$= 0.197 s, for the Pizzoli's town hall (this corresponds instead to mode 3 in Fig. 12, that is the main period in the X direction). The values of these periods were identified through an input-output analysis using the time-histories recorded during these two mainshocks in Cattari et al. (2021) and in Cattari et al. (2018), for the former courthouse and the town hall, respectively. If compared with the dynamic parameters identified under operational conditions, these values are higher. In fact, it can be observed that, in both cases, frequencies decrease systematically with the increase of the amplitude of the shaking at base for all the principal structural modes of the building (Michel and Guéguen, 2010; Lorenzoni et al., 2019; Cattari et al., 2021; Martakis et al., 2022).

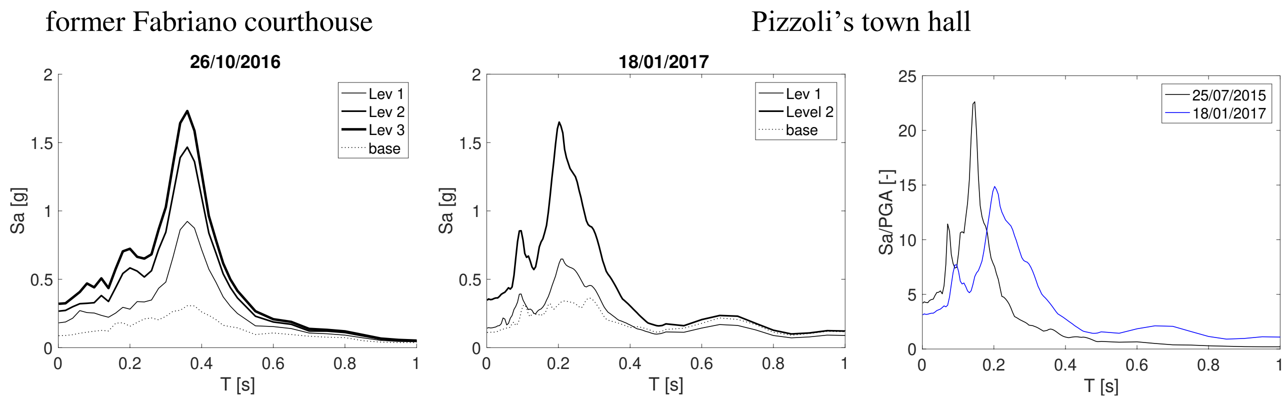

a) b)

Fig. 4a) Amplification phenomenon recorded by the monitoring system on the former Fabriano courthouse (main event of 26/10/2016-19:18) and on the Pizzoli's town hall (main event of 18/01/2017); b) Effects of nonlinearity on the floor spectra shape for the Pizzoli town hall.

For the Pizzoli's town hall, Fig. 4b) shows the effects of the nonlinearity on the floor spectra shapes. To this aim, the floor spectrum (normalized to the *PGA*) obtained after a minor event (in black) is compared with that derived from the main shock of 18/01/2017 (in blue). Actually, the floor spectra obtained from i*n-situ* measurements have shapes more irregular than those obtained from the experimental tests mentioned in §1, but anyhow the same trend can be recognized (see for example Beyer et al., 2015). Indeed, in the case of experimental campaign carried out on shaking table, the same record was scaled at the base up to inducing increasing damage in the prototype: thus, this trend emerged in a more systematic way from the results of the experimental campaign. Conversely, interpreting the same phenomenon on existing buildings is more difficult, since the floor spectra come from different seismic events and it is known a dependence of its shape on the frequency contents and characteristics of the ground motion as well (Rodriguez et al., 2021). However, one can observe that, with increasing nonlinearity of the building, the main structure amplifies the ground motion around elongated periods. This is clear for the town hall in Pizzoli that exhibited a moderate level of damage. In fact, it is possible to see a peak of spectral acceleration around $T_{1,X}$=0.153 s (mode 3 as identified under operational condition - Fig. 12) when the floor spectrum is obtained before the Central Italy earthquake; instead, this peak is reduced and in correspondence of a higher value of $T_{1,X}$= 0.197 s, as it is possible to observe from the floor spectrum evaluated during the mainshock of 18/01/2017.

4 Basics of the practice-oriented floor spectra formulation proposed by the Authors

The expression applied in this paper to analytically compute the floor spectra was the one originally proposed by the Authors in Degli Abbati et al. (2018). The interested reader can refer to the original publication for all the details while the main basics of the proposal are briefly recalled below.

The expression follows a floor spectrum approach, that is based on the simplified assumption to neglect the dynamic interactions between primary and secondary structures. It was verified that this assumption is licit when the secondary element has a negligible mass with respect to the one of the primary system (Degli Abbati et al., 2018; Muscolino, 1991). The expression allows to evaluate the seismic input in terms of floor spectra in different points of the building and at different levels, by properly combining the contribution of the relevant modes. The expression is easy-to-use, because it depends on few parameters, that are: the seismic input at the base, expressed in terms of response spectrum; the main dynamic parameters of the selected modes; the damping features of the main structure and of the secondary element/local mechanism to be verified. These data can be obtained directly from a numerical structural model or applying simplified expressions available in literature and codes (Degli Abbati et al., 2017; Degli Abbati et al., 2021b).

Eq. (1) summarizes the used expression, which gives the acceleration floor spectra at the level Z of the main structure (where the element to be verified of period T and damping ξ is placed) as:

$$S_{a,Z}(T,\xi) = \sqrt{\sum_{k=1}^{N} S_{aZ,k}^{2}(T,\xi)} \qquad (\geq S_a(T)\eta(\xi) \quad \text{for} \quad T > T_1) \tag{1}$$

where $S_a(T)$ is the acceleration response spectrum of the ground motion, N is the number of considered modes and $S_{aZ,k}(T,Z)$ is the contribution of the k^{th} mode that is given by:

$$S_{aZ,k}(T,\xi) = \begin{cases} \dfrac{AMP_k\, PFA_{Z,k}}{1 + [AMP_k - 1]\left(1 - \frac{T}{T_k}\right)^{1.6}} & T \leq T_k \\[2ex] \dfrac{AMP_k\, PFA_{Z,k}}{1 + [AMP_k - 1]\left(\frac{T}{T_k} - 1\right)^{1.2}} & T > T_k \end{cases} \tag{2}$$

In particular, in Eq. (2):

- $PFA_{Z,k}$ is k^{th} peak floor acceleration that depends on the modal parameters of the main structure in terms of natural periods (T_k), modal participation coefficients (Γ_k) and modal shapes ($\Phi_k\ (X\ Y\ Z)$) and its viscous damping ξ_k. Furthermore, it depends on the ground spectrum $S_a(T_k)$ calculated in correspondence of the structure natural period T_k and properly reduced through the damping correction factor $\eta(\xi_k)$:

$$\mathrm{PFA}_{Z,k}=S_a(T_k)\eta(\xi_k)|\Gamma_k\Phi_k|\sqrt{1+4\xi_k^2} \tag{3}$$

- AMP_k is an amplification factor of the $PFA_{Z,k}$, defined by two contributions: f_k that depends only on the viscous damping of the main structure, and f_s that depends only on the one of the secondary element. The expressions proposed to calculate f_k and f_s are:

$$f_k = \xi_k^{-0.6} \tag{4}$$

$$f_s = \eta(\xi) = \sqrt{\frac{0.1}{0.05+\xi}} \geq 0.55 \tag{5}$$

The damping ξ_k associated to the main structure allows to account for the regime in which it works, if still pseudo-elastic or nonlinear. More specifically, it is possible to consider its nonlinear behavior through an equivalent nonlinear system, taking into account the period elongation and an increased damping ξ_k of all the modes for which the nonlinearity occurs.

4.1 Criteria adopted for the validation of the floor spectra formulation

In order to validate the expression recalled at §4, the experimental floor spectra obtained from the monitoring system were compared with the analytical ones. While the first ones were evaluated through a step-by-step integration of the floor acceleration time histories recorded by the sensors at each story, the second ones were computed by using the parameters hereinafter defined:

- the response spectrum at the ground floor calculated in correspondence of the structural natural periods - namely, $S_a(T_k)$ - was determined from the accelerations applied to the structure and recorded by the three-axial sensor at the base. In particular, in both case-studies, $S_a(T_k)$ were computed as the integral in a proper range of periods around T_k, assumed equal to $T_k \pm 0.06$ s. This was done to reduce the sensitivity to the estimation of T_k that is usually present when the floor spectra are computed starting from a response spectrum derived from an actual record. In fact, the latter is characterized by an irregular shape due to the presence of peaks and valleys (see for example the response spectra at the foundation in Fig. 4a); thus, the value of $S_a(T_k)$ can significantly differs if the computation of $S_a(T_k)$ occurs in correspondence of a peak or a valley.
- All the structural dynamic parameters were directly obtained from a modal analysis performed on the calibrated EF models, once selected the number of modes considered representative to describe the structural response. This is coherent with the procedure typically followed in the engineering practice, where monitored data are usually not available, and the practitioner evaluates the necessary parameters from a numerical model.

– The damping factor of the building ξ_k, associated to each mode, was instead evaluated following a two-step procedure. Firstly (a), the structural damping was obtained from the experimental data in order to guarantee the best fitting in terms of peaks between analytical and measured floor spectra. In particular, it was obtained for each sensor and on the dominant mode. The dominant mode is the one characterized by the major contribution in terms of the product P (Eq. (6)) normalized to the maximum one (hereinafter defined P_{norm}). Then (b), it was determined only a value for each mode, evaluated as the mean of the damping factors obtained in the previous step.

$$P = S_a(T_k)|\Gamma_k \phi_k(X, Y, Z)| \tag{6}$$

– finally, a damping factor ξ equal to 5% was assumed in all cases, since the aim of the paper was to evaluate the seismic input for the verification of an atop non-structural element assumed to be still in an elastic phase.

5 Application to the former Fabriano courthouse

5.1 Assessment of data used as input for the analytical computation of floor spectra

This section presents how the parameters necessary to analytically compute the floor spectra were evaluated for the former Fabriano courthouse.

The ground response spectrum was computed from the accelerations recorded by the sensors n.29 and n.30 placed at the building foundation (Fig. 1a). In particular, the recordings of the secondary event of the 19th April 2014 (with PGA_X= 0.00126g and PGA_Y= 0.00136g) and of the main shock of 26th October 2016 - 19:18 (PGA_X= 0.082g; PGA_Y= 0.088g) were used.

The contribution of the first eight modes was considered, since the building has a quite irregular in plan configuration and it is expected that the dynamic response could be affected also by the presence of higher modes. Fig. 5 shows the modal shapes obtained from the numerical model of the first four modes, that are the ones activating the most significant participant mass (overall close to 70%). In particular, the first (T=0.293 s) and second (T=0.286 s) modes activate the transversal response of the two wings in the Y direction, the third mode (T=0.226 s) is in the X direction, while the fourth mode (T=0.191 s) is torsional.

For each mode, to apply the expression of §4, it is necessary to compute the periods, the modal shapes and the participation coefficients, assumed as described below.

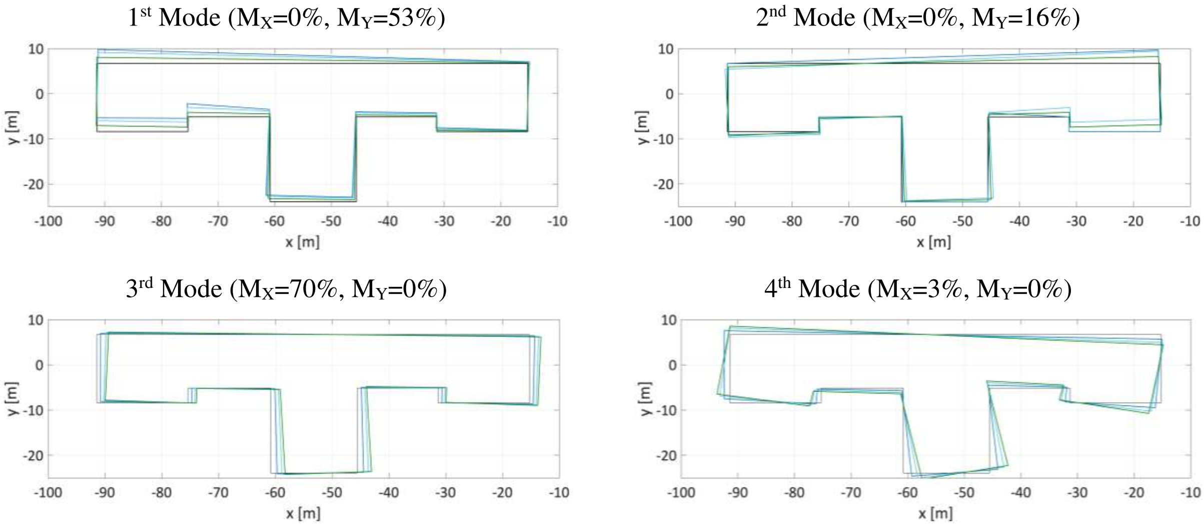

Fig. 5 Numerical modal shapes of the first four modes of the former Fabriano courthouse (each color refers to a different story).

As far as the periods concern:

- for the floor spectra evaluation of the secondary event, the numerical periods obtained from the modal analysis of the model calibrated in the elastic field were used;
- instead for the mainshock, the periods used were those identified in Cattari et al. (2021) using the examined seismic event (namely, E3 in Table 1) and employing the CSI input–output technique. The input was represented by the signals measured from the three-axial sensor at the base of the structure, while outputs were the response of the building which were recorded by sensors installed at the different storeys.

In fact, despite after the earthquake the building response was in the pseudo-elastic field (as also numerically confirmed by the nonlinear dynamic analyses), the frequency identified during different mainshocks and aftershocks present a noticeable variation across the entire set of observed seismic events, as one can see from Table 1 (adapted from Cattari et al., 2021).

Table 1. Frequencies [Hz] identified during the seismic events (table adapted from Cattari et al., 2021)

Modes	**Event ID**									
	E1	**SE1**	**E2**	**E3**	**SE2**	**E4**	**SE3**	**AN**	**E5**	**SE4**
1	3.20	-	3.30	2.36	-	2.40	-	3.37	2.81	3.16
2	-	3.91	-	-	3.46	2.81	3.17	3.60	3.23	3.52
3	4.31	4.78	4.24	3.91	4.34	3.48	4.29	4.44	4.26	4.50
4	4.63	5.33	4.82	4.05	4.82	3.99	4.58	4.91	4.90	5.06
5	-	5.53	-	-	-	4.37	4.88	5.39	5.09	5.42
6	5.12	5.94	-	-	5.37	-	5.00	5.61	-	5.52
7	5.82	6.83	-	-	-	-	-	6.61	5.93	6.87
8	6.63	-	6.79	-	6.89	5.74	6.26	7.51	6.51	-

Abbreviations: E: mainshock; SE: secondary event; AN: ambient noise

E1: 24/08/2016 01:36; E2: 26/10/2016 17:10; E3: 26/10/2016 19:18; E4: 30/10/2016 06:40; E5: 18/01/2017 10:14
SE1: 08/10/2016 18:11; SE2: 28/10/2016 13:56; SE3: 03/11/2016 00:35; SE4: 03/02/2017 05:40; AN: 07/12/2016 15:14

In general, the maximum frequency values (for all the vibration modes) can be observed from the analysis of the ambient noise (AN in Fig. 6a), even if this record was acquired after the most significant seismic events of the earthquake swarm. Furthermore, the frequencies tend to decrease with increasing maximum *PGA* recorded at the building base, following an inverse linear correlation (Fig. 6b), even if no damage was detected on the structure. This frequency wander in buildings is a phenomenon well-known in literature (Clinton, 2006; Celebi, 2007; Ceravolo et al., 2017), that can be observed with or without structural damage, in case of strong earthquakes and also during weak forced vibrations and seismic motions (Spina and Lamonaca, 1998; Ceravolo et al., 2017), where it may be governed by the frequency characteristics of the input (Michel and Gueguen, 2010). In particular, it is an amplitude-dependent phenomenon, that can be composed of a transient (reversible) contribution and a permanent (irreversible) contribution. As already highlighted by Ceravolo et al. (2017) and Lorenzoni et al. (2013), the reversible phenomenon is mainly ascribable to many sources, *e.g.* reversible material and geometrical nonlinearities, SSI, interaction between structural and non-structural elements. Indeed, if no structural damage occurs, the frequency shift gradually vanishes in time and the pre-seismic values of natural frequencies are completely recovered.

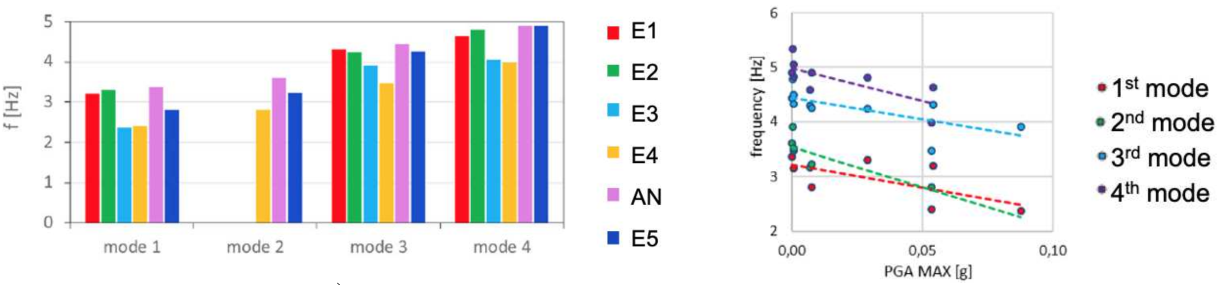

a) b)

Fig. 6 a) Natural frequencies wandering of the first four modes obtained by data analysis from main shocks and ambient vibrations; b) Seismic wandering of the modal frequencies as a function of *PGA*. A linear fitting of data is assumed (figures adapted from Cattari et al., 2021).

Concerning the modal shapes and the participation coefficients, they were assessed from the calibrated EF model, by assuming no change in the modal shapes during the seismic shock of 26th October 2016. The latter assumption is licit as demonstrated by the modal displacement at the nodes where sensors are installed that keep unchanged, meaning that no significant variation of the corresponding mode shapes occurred (Cattari et al., 2021).

Table 2 collects the values of periods used in the floor spectra computation and the damping used for each mode and for each seismic event; the latter was obtained from the two-step procedure described at §4.1. It has to be pointed out that, for the modes from 4 to 8 (*i.e.* those with a negligible contribution in terms of product P as better clarified in the following) the damping was assumed equal to 5%. The values obtained for the other modes are around 5%, as expected in the elastic or pseudo-elastic response; only for mode 3 and in the mainshock of October a higher value was obtained. However, this result is in line with the experimental damping (see ξ_{exp} in Table 3, evaluated as the ratio between the peak and the PFA_{exp}) and with the damping identified with input-output analysis (even if the latter are in general lower).

Table 2. Periods and structural damping used for each mode in the floor spectra evaluation (step 2)

Event	**Input data**	**Mode 1**	**Mode 2**	**Mode 3**	**Mode 4**	**Mode 5**	**Mode 6**	**Mode 7**	**Mode 8**
19th April 2014	T_k [s]	0.293	0.286	0.226	0.191	0.139	0.136	0.128	0.108
	ξ_k [%]	5	4	5	5	5	5	5	5
26th October 2016	T_k^* [s]	0.424	0.356	0.256	0.247	0.186	0.178	0.151	0.133
	ξ_k [%]	4	5	10	5	5	5	5	5

* **Note:** Periods identified with the examined event (E3 in Table 1) using input-output analysis. Modes from 5 to 8 (not identified during the mainshock) are the one obtained from the analysis of the ambient noise (AN in Table 1) acquired after the earthquake swarm.

5.2 *Floor spectra evaluation*

Fig. 7 shows the *PFA/PGA* profiles along the longitudinal direction and for the sensors placed along the same vertical alignments (VA as identified on the axonometry in Fig. 9). The dashed plots refer to the values of *PFA* analytically obtained and compared with the experimental ones (continuous plots).

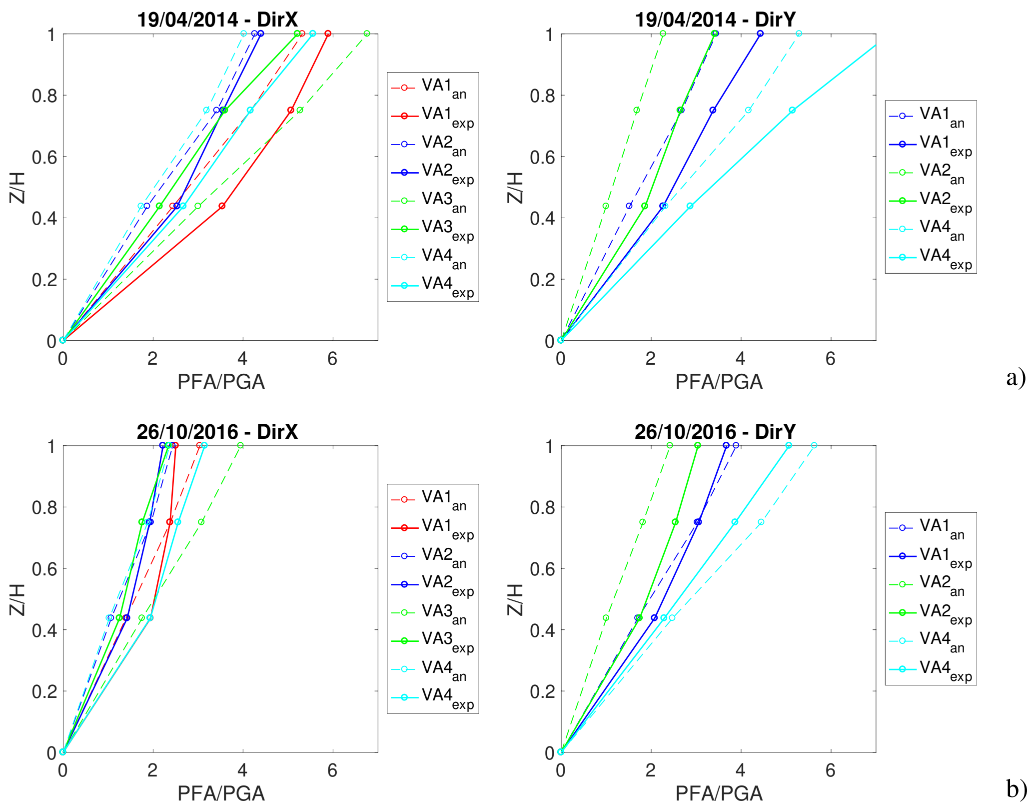

Fig. 7 *PFA/PGA* profile along the height of the building: comparison between analytical (dashed plot) and experimental profiles (continuous plot) for the two examined seismic events: a) minor event of 19/04/2014 and b) mainshock of 26/10/2016.

Some considerations can be drawn:

- the maximum value of *PFA/PGA* measured by the monitoring system is generally between 2 and 6 and it is registered at the top floors. The amplification is reduced in the X direction of the mainshock, while it is quite similar comparing the two events in the Y direction;
- analytical profiles tend generally to underestimate the experimental ones;
- despite the complexity of the building, the shape of the profiles is roughly linear for all the VAs, since the dynamic response of the structure is mainly dominated by the contribution of the fundamental modes in the two main directions (mode 3 in the X direction and modes 1 and 2 in the Y direction – see also Table 3).

Fig. 8 instead illustrates, for both the seismic events and for each sensor, the comparison between the experimental and analytical values of *PFA* (Fig. 8a); moreover, also the periods *T* are reported (Fig. 8b). In particular, the analytical *PFA* are evaluated alternatively considering only the contribution of the dominant mode (*i.e.* the one characterized by the highest value of the product *P* - Eq. (6) in §4) or combining the contribution of the selected modes with a SRSS rule. The analytical plots of *PFA* are respectively colored in blue and magenta, while the experimental ones are in red. Fig. 14a is drawn on a semi-logarithmic scale for more clarity. Instead, in Fig. 14b, the experimental periods (in red) are those evaluated in correspondence of the maximum recorded spectral acceleration peaks, while the analytical ones (in blue) are those which correspond to the modes with the highest contribution again in terms of *P*. It has to be recalled that the sensors underlined on the X-axis in Fig. 8b are the ones in the X direction. The sensors placed at the foundation level (from 1 to 7) are not reported, since not interesting within the aims of this paper.

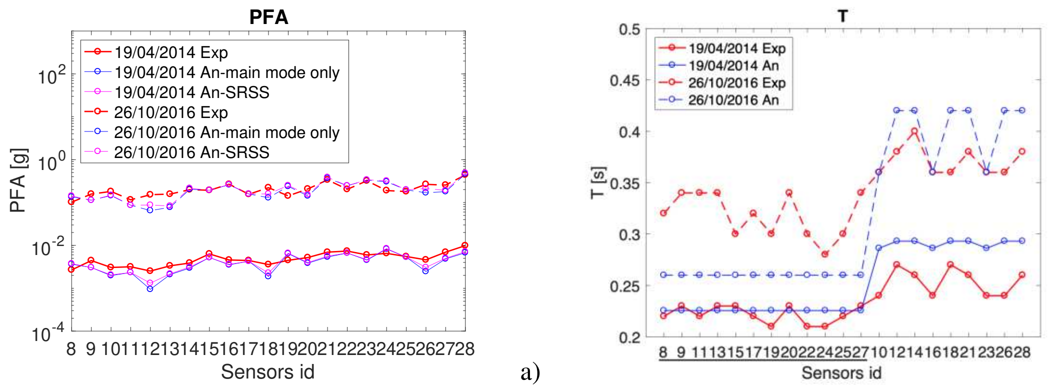

b)

Fig. 8 Comparison, for each sensor and for the two considered events, between: a) analytical and experimental *PFA*; b) analytical and experimental periods *T*.

From this figure, it is possible to see that:

- the major contribution to the floor spectra is due to the fundamental mode in the direction of analysis for all the sensors except for the ones aligned along VA2y (sensors n. 12, 18 and 26): here, in fact, the dominant mode is mode 1, but the dynamic response is also affected by the contribution of mode 2, even if to a lesser degree (P_{norm} around 60% - see Table 3);

- the correspondence between analytical and experimental periods is quite good for both the events in the Y direction and for the minor event in the X direction, while the analytical periods underestimate the experimental ones in the X direction and for the mainshock;
- passing from the minor to the main event, it is possible to observe a period elongation, due to the "co-shift" phenomenon already described in §5.1.

Fig. 9 shows instead the comparison between the recorded (continuous plot, labelled as "exp") and analytical (dashed plot, labeled as "an") acceleration floor spectra for the two events at the sensors located along the same VA. In this case, the experimental floor spectra are characterized by irregular shapes, probably due to the major complexity of this case-study. However, the comparison appears satisfying.

Table 3 shows the damping factor obtained for each sensor from the experimental data (step 1 of the procedure explained at §4.1). It has to be specified that the values of ξ_{fit}, ξ_{exp} and PFA/PFA_{exp} presented in brackets refer to the mainshock of 26th October 2016, while the others to the minor event of 19th April 2014. In particular, the table collects, for each sensor and VA:

- the dominant mode;
- the secondary mode, that was the one characterized by a contribution in terms of P_{norm} respectively higher than 60% (if the number in the table is positive) or higher than 30% (if the number is negative);
- the fitted structural damping (ξ_{fit}), obtained to guarantee for each sensor the best fitting between the analytical peak determined on the dominant mode and the experimental one;
- the experimental structural damping (ξ_{exp}), obtained from the ratio between the experimental peak and the experimental *PFA*;
- the ratio between analytical and experimental *PFA*.

Concerning the ratio PFA/PFA_{exp}, it has to be pointed out that when this ratio is higher than one, it means that the numerical calibrated model (from which the values of Γ and Φ were calculated) overestimates the experimental response. Thus, a higher damping factor is necessary to compensate for this overestimation. On the contrary, if the ratio is lower than 1, the experimental response is underestimated, and the fitted structural damping is lower. In other words, when the PFA/PFA_{exp} ratio is around 1, it means that the numerical model catches well the experimental response; as a consequence, ξ_{fit} is almost equal to ξ_{exp}. This would be completely rigorous if ξ_{exp} would be evaluated as the ratio between the peak and the contribution of the *PFA* due to that mode; otherwise, when the *PFA* is influenced by many modes, the obtained damping is overestimated, because the experimental ratio becomes lower than that one we would use to evaluate ξ_{exp}. Thus, when the floor spectrum is influenced by the contribution of many modes, the ratio PFA/PFA_{exp} is affected by the underestimation of ξ_{exp}, as well.

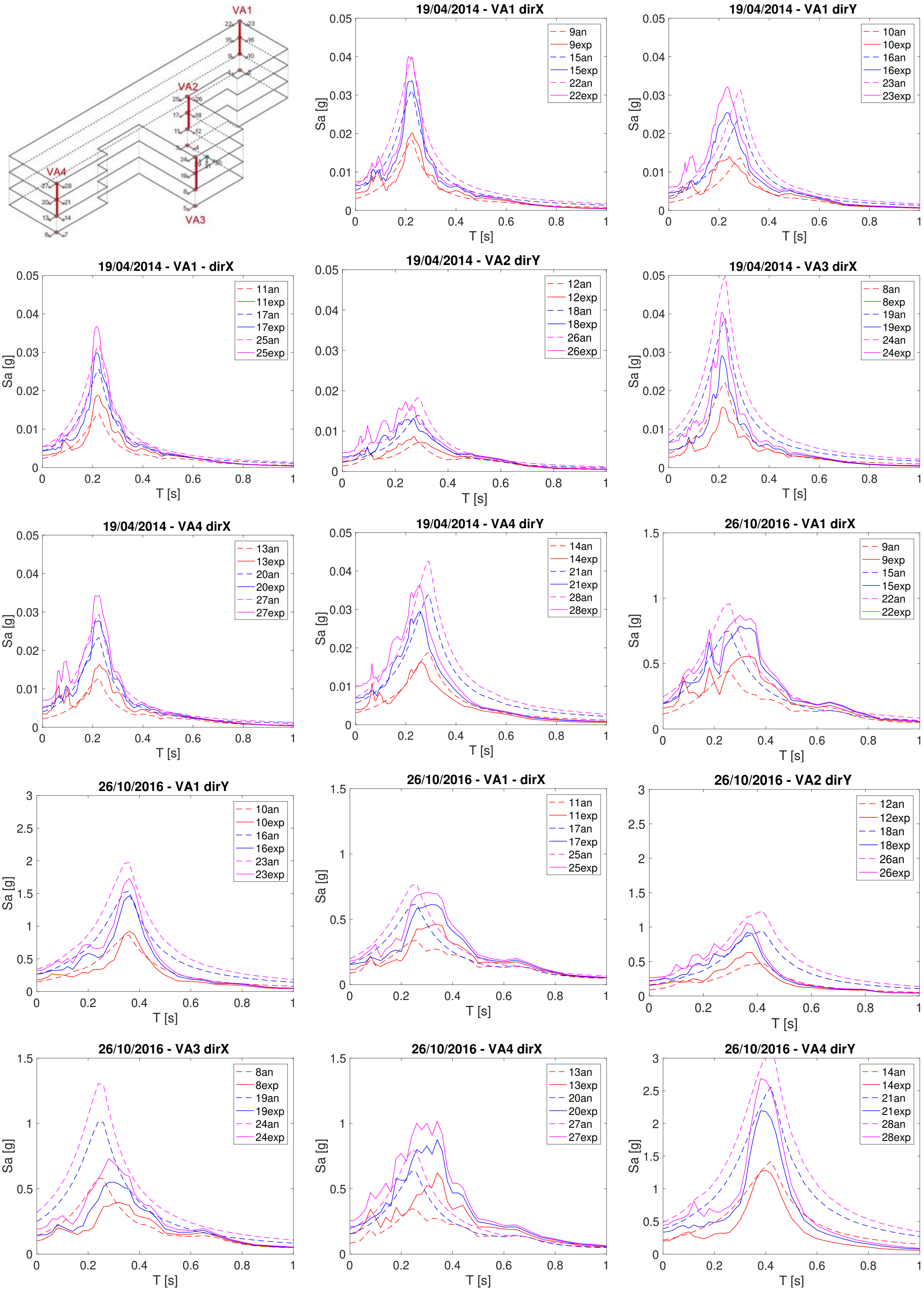

Fig. 9 Floor spectra for the minor event of 19/04/2016 and the mainshock of 26/10/2016: comparison between experimental (continuous plot) and analytical ones (dashed plot).

As one can see from the table, for the sensors placed in the X direction, the dominant mode is usually mode 3, while for the sensors in the Y direction, the dominant modes are mode 1 (for the sensors placed along VA2 and VA4) and mode 2 (for the sensors placed along VA1). Moreover, sometimes the response is also affected by higher modes, whose contribution can affect more (as for VA2y) or less (as for VA4x and VA4y) the final floor spectra. For example, this is evident from Fig. 10 for the sensor 12 where a not negligible contribution is due to modes 1 (the dominant mode) 2, 8 (secondary modes with P_{norm} higher than 60%) and 7 (secondary mode with P_{norm} lower than 30%).

Table 3. Damping evaluation for each sensor (step 1): secondary event of 19th April 2014 and mainshock of 26th October 2016 (values in brackets).

Dir X	Level	Sensor id	Dominant mode	Secondary mode	ξ_{fit} [%]	ξ_{exp} [%]	PFA/PFA$_{exp}$ [-]
VA1	1	9	3	0	4.4 (7.9)	7.9 (12.2)	0.71 (0.77)
	2	15	3	0	4.6 (9.7)	6.2 (9.6)	0.84 (1.01)
	3	22	3	0	5.0 (11.4)	5.9 (8.9)	0.90 (1.17)
VA2	1	11	3	0	3.5 (7.1)	5.1 (9.9)	0.80 (0.83)
	2	17	3	0	4.2 (10.2)	4.2 (10.2)	1.00 (1.01)
	3	25	3	0	4.2 (11.2)	4.2 (10.2)	1.01 (1.06)
VA4	1	13	3	0 (-4)	3.6 (4.4)	7.1 (10.1)	0.69 (0.64)
	2	20	3	0 (-4)	4.0 (6.1)	6.1 (9.1)	0.80 (0.83)
	3	27	3	0 (-4)	4.1 (6.7)	7.0 (10.0)	0.76 (0.83)
VA3	1	8	3	0	7.4 (14.0)	5.3 (10.4)	1.27 (1.28)
	2	19	3	0	6.9 (18.2)	4.5 (10.5)	1.35 (1.50)
	3	24	3	0	6.3 (17.6)	4.8 (10.6)	1.23 (1.45)

Dir Y	Level	Sensor id	Dominant mode	Secondary mode	ξ_{fit} [%]	ξ_{exp} [%]	PFA/PFA$_{exp}$ [-]
VA1	1	10	2	0	3.8 (4.68)	7.9 (6.6)	0.68 (0.83)
	2	16	2	0	3.8 (5.4)	5.7 (5.8)	0.80 (0.97)
	3	23	2	0	3.9 (5.9)	6.1 (6.0)	0.78 (1.01)
VA2	1	12	1	2,8	3.0 (2.6)	12.7 (9.3)	0.55 (0.60)
	2	18	1	2	4.2 (3.8)	11.5 (9.3)	0.65 (0.72)
	3	26	1	2	4.1 (4.5)	11.1 (10.0)	0.68 (0.78)
VA4	1	14	1	0 (-2)	5.5 (4.4)	9.1 (4.5)	0.79 (1.06)
	2	21	1	0 (-2)	5.6 (4.8)	9.0 (4.4)	0.79 (1.11)
	3	28	1	0 (-2)	5.7 (4.9)	11.4 (4.9)	0.70 (1.07)

It has to be pointed out that, from the analysis of the experimental data, it is quite clear that the structure filters also the frequency in correspondence of the peaks present in the seismic input. This is for example highlighted in the floor spectrum of sensor 22 of Fig. 10, which has two peaks: one at the fundamental period and the other at a lower period with a not negligible frequency content present in the input. Indeed, this aspect cannot be taken into consideration by the proposed formulation, which instead considers the value of the ground response spectrum only at the fundamental periods of the building.

Secondary event of 19/04/2014

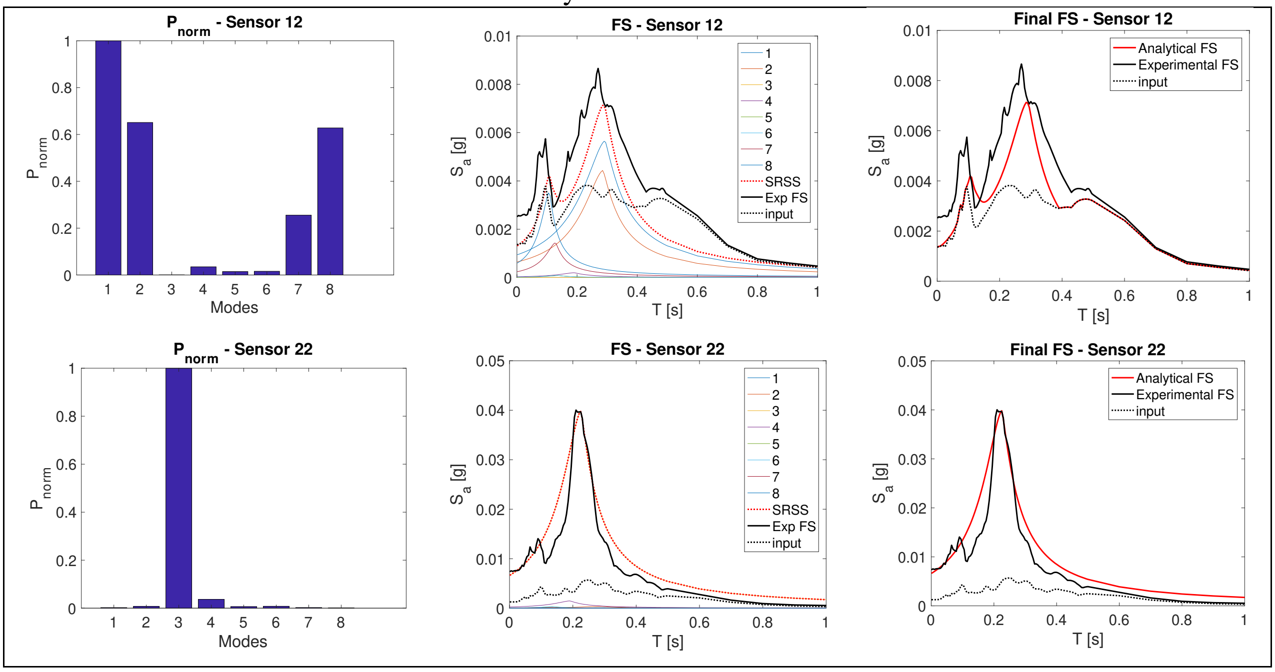

a) b) c)

Fig. 10 a) Contribution of modes in terms of P_{norm}; b) Floor spectra evaluated for each mode; c) Final floor spectra computed with Eq. (1).

Finally, Fig. 11 shows the sensibility of the proposed expression to the choice of the natural periods of the selected modes. Since, as above-mentioned, no appreciable structural damage occurred on the courthouse, it could be considered reasonable also using the modal parameters of the numerical model for the floor spectra evaluation of the mainshock of October 2016. This would be the strategy followed by practitioners, who could not necessarily benefit from the results of the dynamic identification with input-output technique to estimate the structural parameters. The application of the analytical expression with the elastic modal periods obviously would be not able to properly describe the "co-shift" phenomenon of frequency. In Fig.11, the analytical floor spectra evaluated using the modal parameters computed from the numerical Tremuri model (labeled as "Num" – continuous plot) are compared with the ones identified with the examined event (labeled as "Id" – dashed plot). The latter are compared with the experimental ones obtained from the monitoring system (labeled as "Exp" and drawn in red). The comparison is shown for the three VAs with sensors in the Y direction (namely VA1, VA2 and VA4). From Fig. 11, it is possible to see that the floor spectra computed with the periods identified with the seismic event (dashed plot) fit better the experimental ones, which have a maximum amplification peak in correspondence of a period longer than the ones computed from the numerical modal analysis.

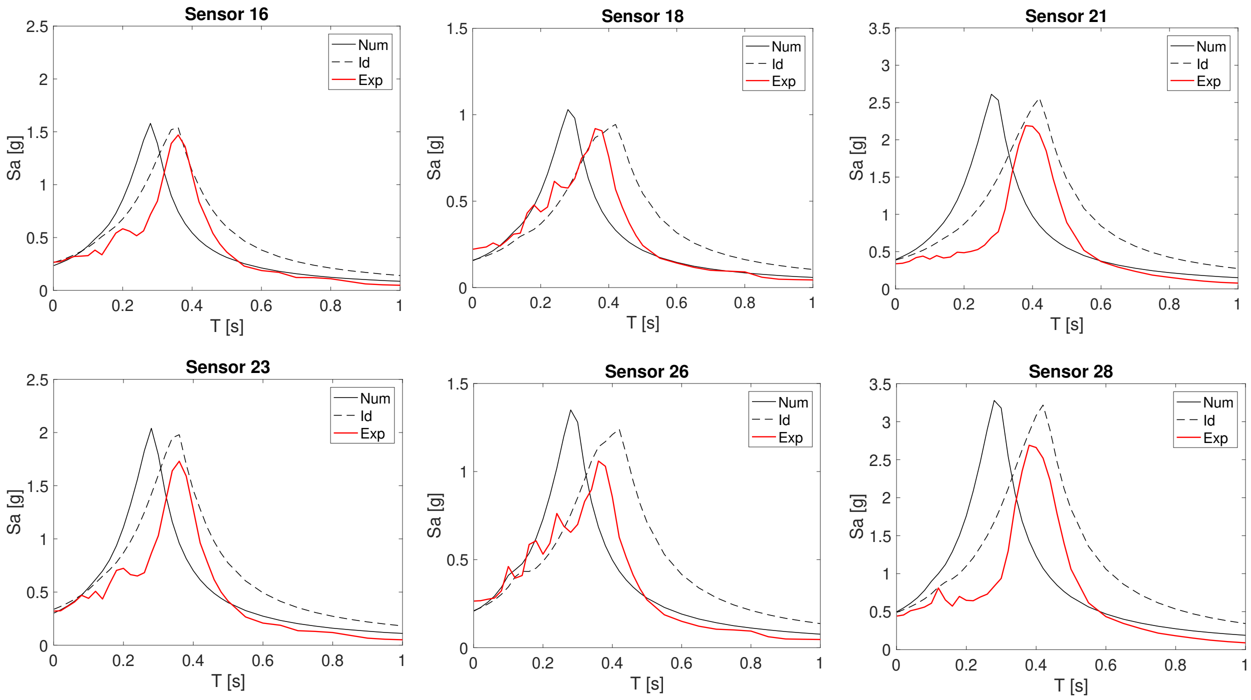

a) b) c)

Fig. 11 Comparison between experimental (labeled as "Exp" and plot in red) and analytical (in black) floor spectra for the mainshock of 26/10/2016. The latter were respectively obtained using: the numerical modal parameters (labeled as "Num" – continuous plot) and the ones identified with the examined event (labeled as "Id" – dashed plot): a) VA1Y; b) VA2Y; c) VA4Y.

6 Application to the Pizzoli's town hall

6.1 Assessment of data used as input for the analytical computation of floor spectra

This section describes the application to the second case-study. In particular, the results will be presented following the same outline already illustrated for the former Fabriano courthouse. In order to avoid repetitions, only the peculiar aspects and the main differences obtained will be commented in the text.

As for the previous case-study, the ground response spectrum was computed from the accelerations recorded by the three-axial sensor placed at the building foundation (sensors n.15 and n.16 of Fig. 1b). In particular, the recordings of the secondary event of the 25th July 2015 (with *PGA* values around 0.001 g) and of the mainshock of 18th January 2017 (PGA_X=0.112g; PGA_Y=0.100g) were used for the floor spectra evaluation.

Unlike the previous case-study, in each direction, the dynamic behavior is dominated by the first translation one (with participant mass higher than 80%, see Fig.12). Despite that, in the floor spectra evaluation the contribution of the first four modes were considered in order to highlight the differences with the former Fabriano courthouse.

Periods, modal shapes and participation coefficients of each mode were computed as follows:

- as far as the periods concern, for the floor spectra evaluation of the secondary event, the numerical periods obtained from the modal analysis performed on the model calibrated in the elastic field were used. Instead, for the floor spectra evaluation of the main shock, the analysis of the occurred damage (Fig. 2) and of the numerical dynamic response simulated during the seismic event (Degli Abbati et al., 2021a) showed that the structural response was in the moderate nonlinear field. Thus, an elongation of the fundamental periods was assumed, coherently also with the experimental evidence (§3). In particular, the elongated periods were computed accounting for a degradation of stiffness properties of masonry. The values were calibrated considering as target the values obtained from the dynamic identification performed by means of input-output techniques by employing the examined recording (ReLUIS projects, Task 4.1 – Cattari et al., 2018);

- concerning the modal shapes and the participation coefficients, also in this case they were assumed from the calibrated EF model developed in Tremuri, by assuming no change produced by damage induced by the seismic shock of 18th January 2017. Again, it was checked that the modal displacements obtained for the different main shocks keep almost unchanged, meaning that no significant variation of the corresponding mode shapes occurred (Cattari et al., 2018; Lorenzoni et al., 2019).

Finally, the damping factor of the building ξ_k (associated to each mode) was evaluated following the two-step procedure already described in §4.1.

Fig. 12 shows the modal shapes of the first four modes obtained from the numerical model. In particular, from the figure, it is possible to see that mode 1 is a translational mode in the Y direction, while mode 3 is a translational mode in the X direction. Table 4 collects instead the values of periods assumed in the floor spectra computation and the damping used for each mode and for each seismic event. For those modes with a negligible contribution in terms of product *P*, a damping equal to 5% was assumed (this is the case of modes 2 and 4). As one can see, the values of damping in Table 4 are coherent with the expected variation in the response, being around 5% in the linear response and a bit higher (around 7%) during the slight nonlinear phase of the response.

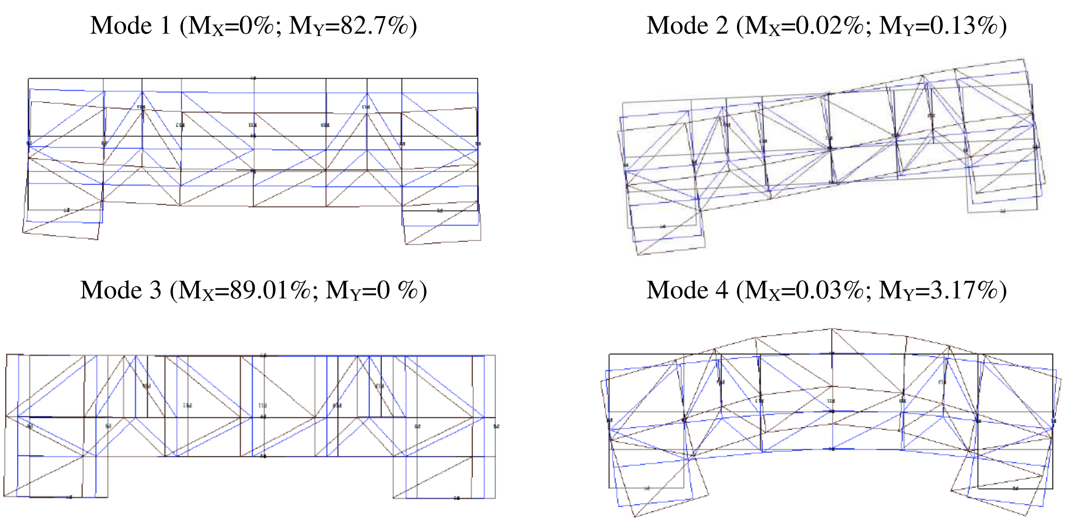

Fig. 12 Numerical modal shapes of the first four modes of the Pizzoli's town hall.

Table 4. Periods and structural damping assumed for each mode in the floor spectra evaluation (step 2)

Event	**Input data**	**Mode 1**	**Mode 2**	**Mode 3**	**Mode 4**
25th July 2015	T_k [s]	0.225	0.181	0.142	0.115
	ξ_k [%]	3	5	5	5
18th January 2017	T_k [s]	0.283	0.224	0.184	0.113
	ξ_k [%]	6	5	7	5

6.2 *Floor spectra evaluation*

Fig. 13 shows the *PFA/PGA* profiles along the longitudinal direction, as obtained from sensors placed along the same vertical alignments (VA as identified on the axonometry in Fig. 16).

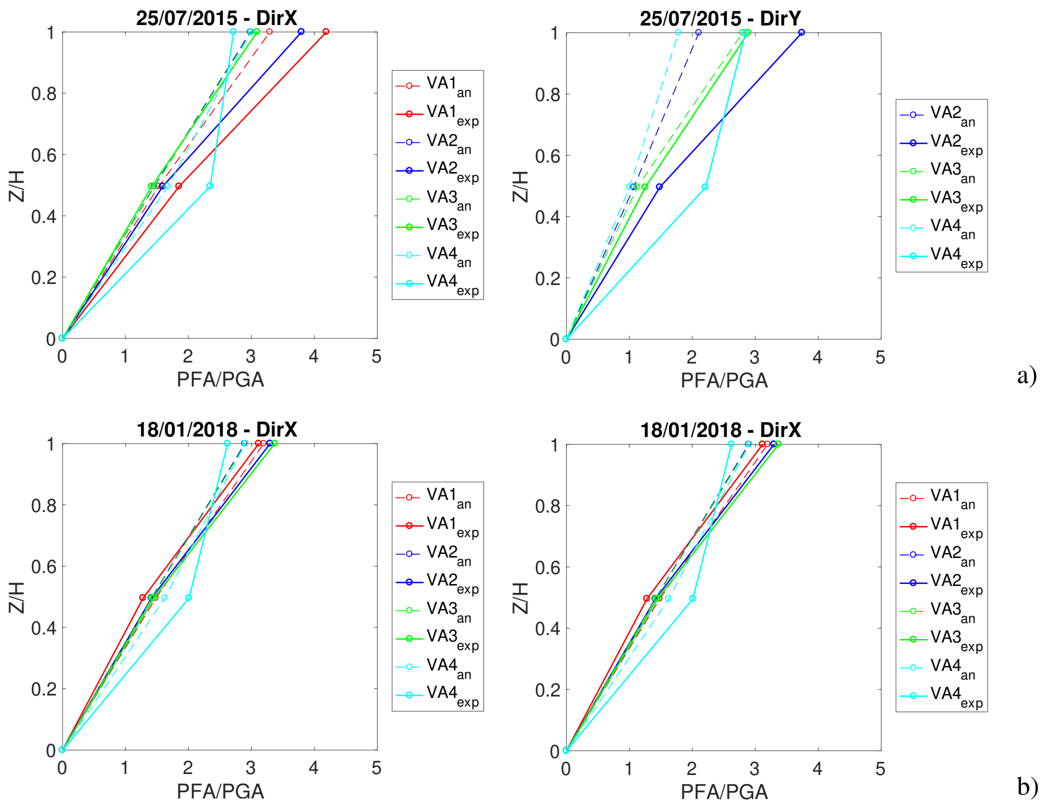

Fig. 13 *PFA/PGA* profile along the height of the building: comparison between analytical (dashed plot) and experimental profiles (continuous plot) for the two examined seismic events: a) minor event of 25/07/2015 and b) mainshock of 18/01/2018.

Comparing these data with the ones obtained for the first case-study, it is interesting to notice that:

- here the maximum value of *PFA/PGA* measured by the monitoring system is generally slightly lower (being between 2.5 and 4), but it is registered again at the top floors; observing the *PFA/PGA* profiles obtained from the recordings of 18/01/2018, it is possible to observe that this amplification is reduced, due to the damage induced by the earthquake on the structure;

- analytical profiles tend to underestimate the experimental ones in both directions for the minor event of 25/07/2015, while they are able to catch the actual profiles in case of the mainshock of 18/01/2017;
- the shape of the profiles differs depending on the considered vertical alignments: it is roughly linear, as expected for a 2-storys building quite regular and with quite stiff diaphragms like the examined one, thus dominated in the dynamic response by the contribution of the fundamental modes in the two main directions. However, it is interesting to observe that this almost linear shape becomes bi-linear for VA2 and VA4: this is probably due to the position of the sensors at the two edges of the plan and, consequently, to the influence of the torsional mode that here is maximum.

Fig. 14 instead illustrates, for the two considered events and each sensor, the comparison between experimental and analytical values of *PFA* (Fig. 14a); also the periods *T* (Fig. 14b) are reported. As for the previous case-study, the sensors underlined on the X-axis in Fig. 14b are the ones in the X direction. From this figure, it is possible to see that:

- the major contribution to the floor spectra is due to the fundamental mode in the direction of analysis (Fig. 14a). For this reason, the analytical *PFA* obtained computing only the main mode (blue plot) and the ones obtained considering the first four modes combined with the SRSS rule are almost identical;
- the correspondence between analytical and experimental periods is quite good, especially for the X direction. Moreover, a period elongation is observed passing from the minor event of 25/07/2017 (continuous plot) to the mainshock of 18/01/2017 (dashed plot) that is properly captured by the analytical expression (Fig. 14b). Only for sensor n.5 the experimental period is significantly lower than the ones detected in the other sensors and analytically evaluated as the period of the mode with the major contribution.

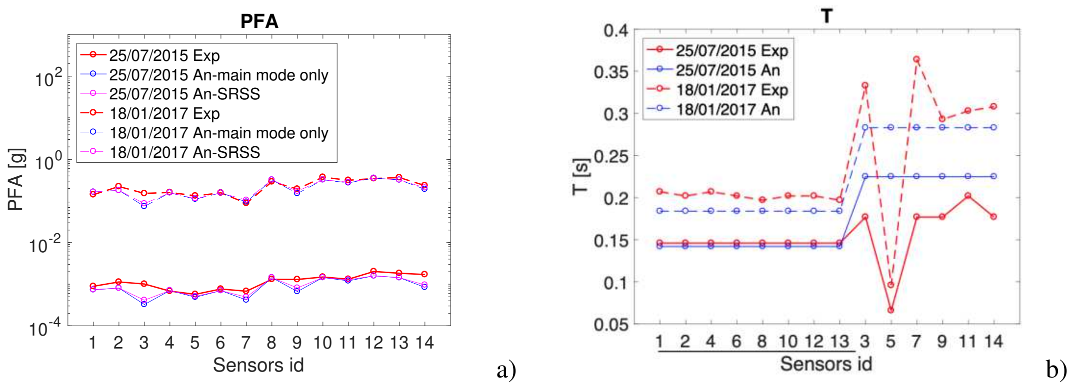

Fig. 14 a) Comparison, for each sensor and for the two considered events, between: a) analytical and experimental *PFA;* b) analytical and experimental periods *T*.

In order to explain the mismatch on sensor n.5, looking at the results presented in Fig. 15b, it is possible to observe that in correspondence of this sensor the structure amplifies the input in correspondence of two range of periods: the first one around T=0.066 s (this is the maximum spectral peak detected in Fig. 14b for the event of 25/07/2015); the second one (which is a bit lower) is instead approximately around the fundamental period in that direction, coherently with what obtained for the other sensors. The same shape characterizes the floor spectrum of the sensor obtained during the event of 18/01/2017 (see Fig. 15c). However, in this case, the two periods with the maximum values of amplification are: T=0.096 s and T=0.3 s; the latter is plausibly the fundamental period, elongated due to the structural nonlinearity. Indeed, it is interesting to observe that a fifth mode with T=0.082 s was experimentally identified by Sivori et al. (2021) and ascribed to the shear mode which activates the local response of diaphragms. Thus, it seems reasonable to conclude that in correspondence of position of sensor n.5, the Pizzoli's town hall filters the ground motion in correspondence of two frequencies: the one which characterizes its global dynamic response and the one which characterizes the local response of diaphragms.

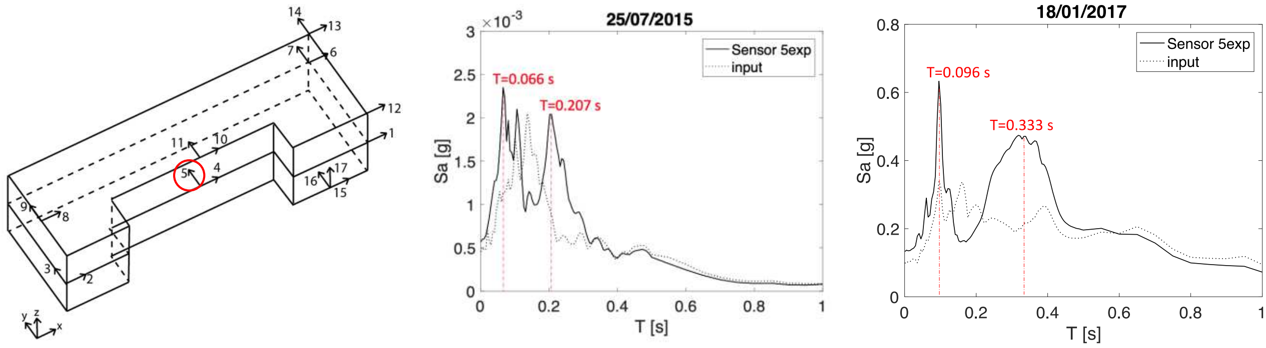

a) b) c)

Fig. 15 a) Sensor 5 location; Experimental floor spectra and identification of the maximum peaks: b) minor event of 25/07/2015; c) mainshock of 18/01/2018.

Fig. 16 shows the comparison between the recorded (continuous plot, labelled "exp") and analytical (dashed plot, labeled "an") acceleration floor spectra for the two events computed for the sensors located along the same VA at the two levels. It should be pointed out that in the figure VA4 comprises sensors 2-3 at the first level and 8-9 at the second one, even not strictly aligned along the same vertical axis. The comparison shows a very good correspondence.

Finally, analogously with what already presented for the former Fabriano courthouse, Table 5 reports the details of the analyses in terms of: dominant and secondary modes, damping factor for each sensor which guarantee the best fitting with experimental data (ξ_{fit}), experimental structural damping (ξ_{exp}) and ratio PFA/PFA_{exp}. Again, the values in brackets refer to the mainshock of 18th January 2017, while the values directly collected in the table refer to the secondary event of 25th July 2015. As one can see from the table, for the sensors placed in the X direction, it is interesting to observe that the only dominant mode is always mode 3, while for the sensors in the Y direction, the dominant mode is mode 1 and sometimes the sensors is affected by the contribution of mode 4, as well. This can be observed also from Fig. 17, which shows for two sensors placed at the second level of the building (sensor n.12 and n.9): a) the importance of the selected modes in terms of P_{norm}; b) the floor spectra evaluated for each mode; c) the final floor spectra, evaluated by the SRSS combination.

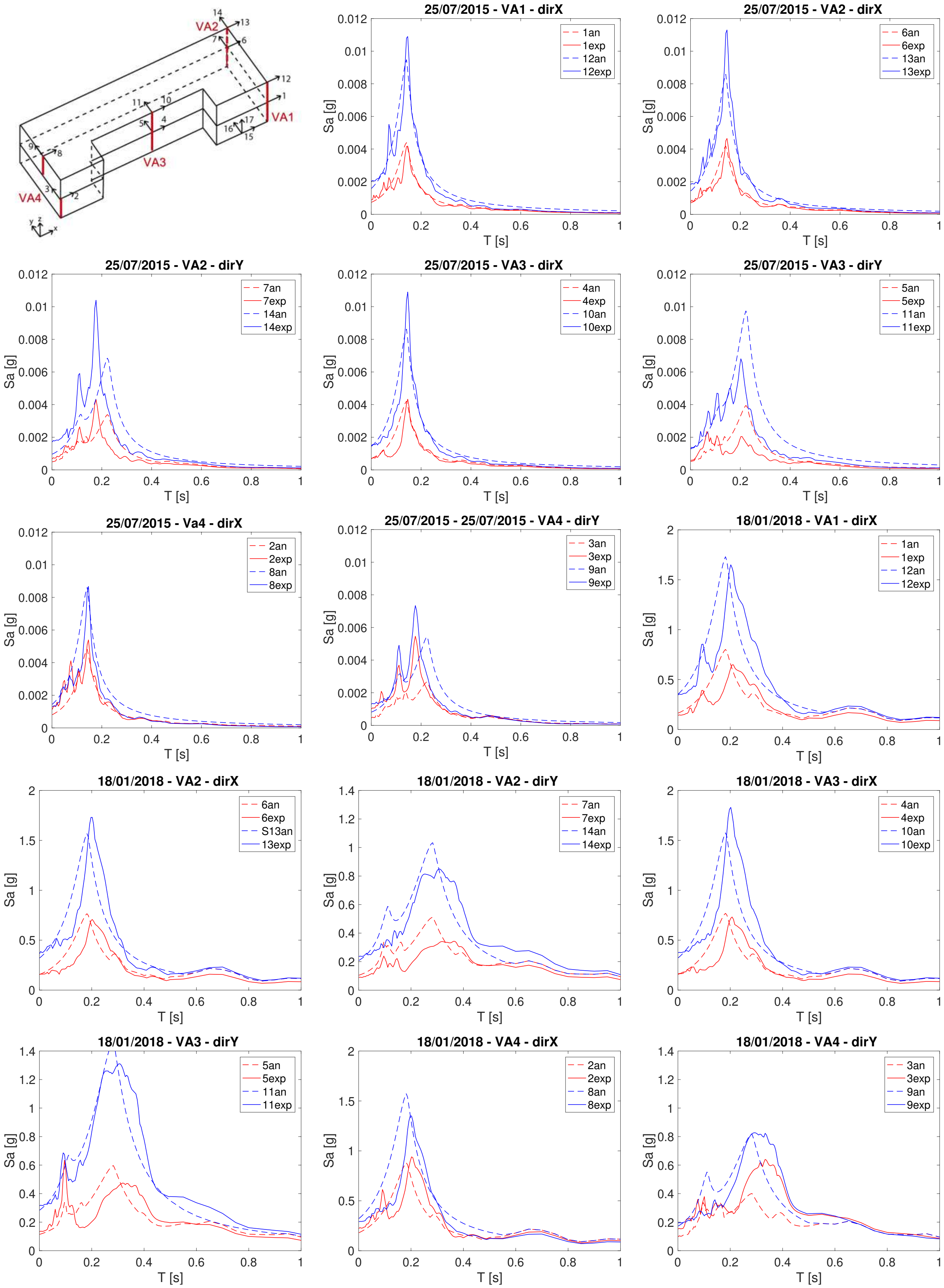

Fig. 16 Floor spectra for the minor event of 25/07/2015 and the mainshock of 18/01/2017: comparison between experimental (continuous plot) and analytical ones (dashed plot).

Table 5. Damping evaluation for each sensor (step 1): secondary event of 25th July 2015 and mainshock of 18th January 2017 (values in brackets).

Dir X	Level	Sensor id	Dominant mode	Secondary mode	ξ_{fit} [%]	ξ_{exp} [%]	PFA/PFA$_{exp}$ [-]
VA1	1	1	3	0	5.3 (9.0)	7.6 (8.0)	0.81 (1.08)
	2	12	3	0	4.2 (7.4)	6.0 (7.4)	0.82 (1.01)
VA2	1	6	3	0	4.4 (7.7)	5.0 (8.1)	0.94 (0.97)
	2	13	3	0	3.6 (6.3)	4.8 (7.5)	0.85 (0.90)
VA3	1	4	3	0	4.9 (7.4)	4.6 (8.0)	1.04 (0.96)
	2	10	3	0	3.8 (5.9)	3.6 (7.1)	1.03 (0.90)
VA4	1	2	3	0	4.4 (6.5)	7.4 (9.1)	0.74 (0.83)
	2	8	3	0	5.0 (8.4)	4.3 (7.7)	1.10 (1.05)

Dir Y	Level	Sensor id	Dominant mode	Secondary mode	ξ_{fit} [%]	ξ_{exp} [%]	PFA/PFA$_{exp}$ [-]
VA2	1	7	1	4	2.2 (9.0)	4.6 (10)	0.75 (1.07)
	2	14	1	4	1.8 (7.0)	4.9 (12)	0.60 (0.84)
VA3	1	5	1	-4	5.7 (6.0)	9.5 (7)	0.79 (0.87)
	2	11	1	-4	4.7 (7.0)	6.5 (9)	0.89 (0.87)
VA4	1	3	1	4	1.2 (3.0)	6.0 (9)	0.45 (0.63)
	2	9	1	4	2.0 (6.0)	5.6 (9)	0.65 (0.89)

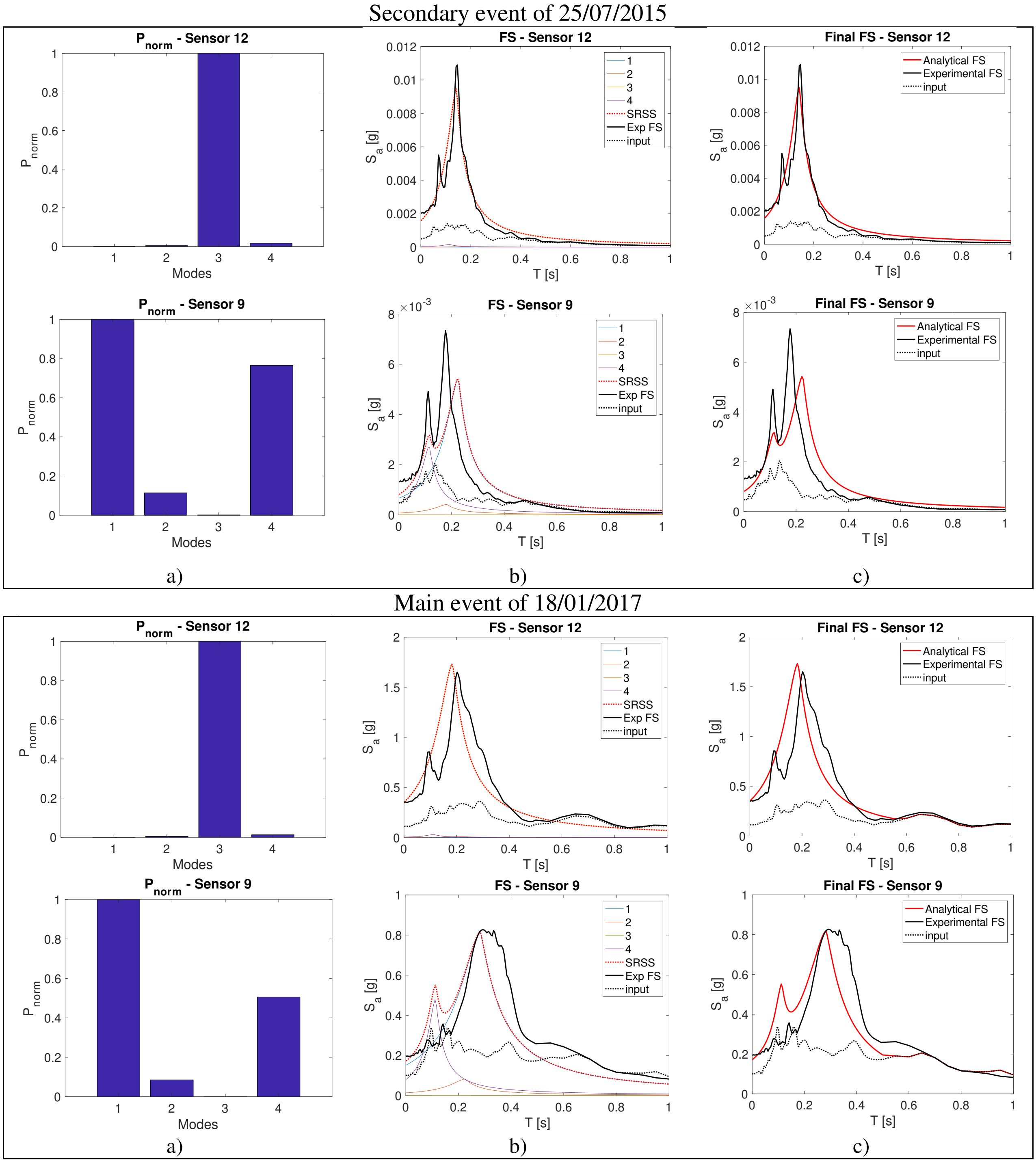

Fig. 17 – a) Contribution of modes in terms of product P_{norm}; b) Floor spectra evaluated for each mode; c) Final floor spectra computed with Eq. (1).

7 Conclusions

Floor spectra are the tools currently prescribed by codes to evaluate the seismic demand on acceleration-sensitive non-structural elements and local mechanisms in masonry buildings. For this reason, the validation of expressions available for their definition can significantly affect the results of seismic assessment procedures and, more generally, the engineering practice.

In this framework, this paper aims to validate a practice-oriented formulation proposed by the Authors in 2018 through the data acquired on two existing URM buildings hit by the last Central Italy earthquake. The two case-studies were selected because interesting for several reasons:

- the buildings were characterized by geometrical configuration of increasing complexity, allowing to investigate also the effects of higher modes contribution on the seismic response;
- dynamic identification data were available for a detailed calibration of numerical models. The numerical models were then used to accurately interpret the dynamic response of these structures through nonlinear dynamic analyses;
- recordings from different mainshocks and minor events were available from the permanent monitoring system and allowed an accurate comparison between measured and analytical floor spectra for the aim of validation of the practice-oriented approach proposed by the Authors;
- the two case-studies exhibited a different damage level after the 2016/2017 Central Italy earthquake, allowing to verify the reliability of the analytical approach both in the linear and moderated nonlinear fields.

The main parameters influencing the shape of floor spectra were identified and discussed in the paper, as obtained by the review of some numerical and experimental studies presented in literature and further corroborated by the analysis of the two investigated case studies. These parameters are the characteristic of the ground motion, the expected *PGA* demand, the dynamic response of the considered building (*i.e.* the vibration periods and the shape of its vibration modes), the lateral load resisting system, the floor level. Floor spectra shape is strongly influenced also by higher vibration modes and by the nonlinearity demand experienced by both hosting and hosted structures. Moreover, other additional parameters, such as diaphragm flexibility or torsional responses, can further amplify the seismic demands on secondary elements.

The expected influence of some of these parameters on floor spectra has been confirmed by the monitoring data acquired by the OSS on the two buildings presented in the paper and by comparing these outcomes with the prediction of the literature formulation proposed by the Authors. The expression turned out to be adequate to properly describe the amplification phenomenon and the effects of nonlinearity. The approach is easy-to-use, because it requires only the basic structural dynamic properties and the expected seismic input. Results have proven that, provided a reliable estimate of dynamic properties, the analytical expression leads to a satisfactory matching with experimental floor spectra both in the linear and moderately nonlinear field. The need of the reliable estimate of dynamic properties highlights the usefulness of the monitoring or ambient vibration tests and that of efficient numerical models.

The recorded data from the two investigated structures showed that the building may amplify the input also in correspondence of those periods characterized by a not negligible spectral content. This aspect is not included in the proposed formulation that only considers the value of the spectral input at the base in correspondence of the natural period of the structure or at least in a small range around it. That could be improved in the future. Moreover, two further area of investigations are identified: the deepening of the co-shift phenomenon, to provide also some easy-to-use approach to estimate it by engineers; a robust validation of the analytical expression also in a strong nonlinear field, possibly supported by nonlinear dynamic analyses carried out on calibrated models (since in this case accurate data on real structures able to document the phenomenon are very rare).

ACKNOWLEDGEMENTS

The results presented in this paper have been obtained within the Italian national research project ReLUIS 2019–2021 (Work Package 6, Coord. Proff M.Savoia and F.Ponzo and Work Package 10, Coord. Prof. G.Magenes) founded by the Italian Civil Protection Agency. Moreover, the results presented in the paper benefited of the data made available by the Italian structural seismic monitoring network (OSS) of the Italian Department of Civil Protection, within the research activities of ReLUIS Project 2017-2018 (WP4 Task 4.1). The authors wish to acknowledge Eng. Daniele Spina for making the OSS data available.

Conflicts of interest

The authors declare that they have no conflict of interest.

Authors' contributions

SDA: Methodology, Formal analysis, Data curation, Visualization, Writing – original draft; SC and SL: Supervision, Writing – review&editing. All authors read and approved the final manuscript.

REFERENCES

Allemange RJ and Brown DL (1982). A correlation coefficient for modal vector analysis, *Proceedings 1st international modal analysis conference*. November 8–10 1982, Orlando, Florida, pp. 110-116.

Anajafi H, Medina RA (2019). Lessons learned from evaluating the responses of instrumented buildings in the United States: the effects of supporting building characteristics on floor response spectra. *Earthq Spectra* 35(1):159–191.

Anajafi H, Medina RA, Santini-Bell E (2019). Inelastic floor spectra for designing anchored acceleration-sensitive nonstructural components. *Bulletin of Earthquake Engineering*, https://doi.org/10.1007/s10518-019-00760-8.

ASCE/SEI 7-10. Minimum Design Loads for Buildings and Other Structures. ASCE 7-10. Reston, VA: ASCE; 2010.

Baggio S, Berto L, Rocca I, Saetta A (2018). Vulnerability assessment and seismic mitigation intervention for artistic assets: from theory to practice. *Engineering Structures* 167: 272-286.

Beyer K, Tondelli M, Petry S, Peloso S (2015). Dynamic testing of a four-storey building with reinforced concrete and unreinforced masonry walls: prediction, test results and data set. *Bulletin of Earthquake Engineering* 13(10): 3015-3060.

Bothara JK, Dhakal RP, Mander JB (2010). Seismic performance of an unreinforced masonry building: An experimental investigation. *Earthquake Engineering and Structural Dynamics,* 39: 45–68.

Brunelli A, de Silva F, Piro A, Sica S, Parisi F, Silvestri F. Cattari S (2021). Numerical simulation of the seismic response and soil-structure interaction for a monitored masonry school building damaged by the 2016 Central Italy earthquake. *Bulletin of Earthquake Engineering* 19(2): 1181-1211.

Calvi PM, Sullivan TJ. Estimating floor spectra in multiple degree of freedom systems (2014). *Earthq Struct* 7(1):17-38.

Cattari S, Degli Abbati S, Ottonelli D, Sivori D, Spacone E, Camata G, Marano C, Modena C, da Porto F, Lorenzoni F, Calabria A, Magenes G, Penna A, Graziotti F, Ceravolo R, Matta E, Miraglia G, Spina D, Fiorini N (2018): Report di sintesi sulle attività svolte sugli edifici in muratura monitorati dall'Osservatorio Sismico delle Strutture, Linea Strutture in Muratura, ReLUIS report (Task 4.1 Workgroup), Rete dei Laboratori Universitari di Ingegneria Sismica. *Technical Report* (in Italian).

Cattari S, Degli Abbati S, Ottonelli D, Marano C, Camata G, Spacone E, da Porto F, Modena C, Lorenzoni F, Magenes G, Penna A, Graziotti F, Ceravolo R, Miraglia G, Lenticchia E, Fiorini N, Spina D (2019). Discussion on data recorded by the Italian Structural seismic monitoring network on three masonry structures hit by the 2016-2017 Central Italy Earthquake. *7th ECCOMAS Thematic Conference on Computational Methods in Structural Dynamics and Earthquake Engineering,* Crete, Greece.

Cattari S, Degli Abbati S, Alfano S, Brunelli A, Lorenzoni F, da Porto F (2021). Dynamic calibration and seismic validation of numerical models of URM buildings through permanent monitoring data. *Earthquake Engng Struct Dyn* 50:2690–2711. https://doi.org/10.1002/eqe.3467.

Chen Y, Soong TT (1988). State of art review seismic response of secondary systems. *Engineering Structures*, 10: 218-228.

Celebi M. (2007). On the variation of fundamental frequency (period) of an undamaged building—a continuing discussion. *Proceedings of the Conference on Experimental Vibration Analysis for Civil Engineering Structures* October 24–26, Porto, Portugal. 317-326.

Ceravolo R, Matta E, Quattrone A, Zanotti Fragonara L. (2017). Amplitude dependence of equivalent modal parameters in monitored buildings during earthquake swarms. *Earthquake Engng Struct Dyn* 46:2399-2417.

Commentary of the Italian Technical Code (2019). Circolare esplicativa delle Norme Tecniche per le Costruzioni. Supplemento ordinario n. 5 Gazzetta Ufficiale 11 febbraio, 2019. (in Italian).

Clinton J. (2006). The observed wander of the natural frequencies in a structure. *Seismol Soc Am Bull*. 96(1):237-257.

CESMD [Center for Engineering Strong-Motion Data]. 2019. Accessed May 8, 2019. https://strongmotioncenter.org/.

de Silva F, Piro A, Brunelli A, Cattari S, Parisi F, Sica S, Silvestri F (2019). On the soil–structure interaction in the seismic response of a monitored masonry school building struck by the 2016–2017 Central Italy earthquake. *7th ECCOMAS thematic conference on computational methods in structural dynamics and earthquake engineering*, 24–26 June 2019, Crete, Greece.

Degli Abbati S, Cattari S, Lagomarsino S (2017). Proposta di spettri di piano per la verifica di elementi non strutturali e meccanismi locali negli edifici in muratura. *Proceedings ANIDIS – L'Ingegneria Sismica in Italia*, September 17-21–2017, Pistoia, Italy (in Italian).

Degli Abbati S, Cattari S, Lagomarsino S (2018). Theoretically-based and practice-oriented formulations for the floor spectra evaluation. *Earthquake and Structures*, 15(5), 565-581. DOI: 10.12989/eas.2018.15.5.565

Degli Abbati S, Morandi P, Cattari S, Spacone E (2021a). On the reliability of the equivalent frame models: the case study of the permanently monitored Pizzoli's town hall. *Bull Earthquake Eng*. https://doi.org/10.1007/s10518-021-01145-6.

Degli Abbati S, Cattari S, Lagomarsino S, Ottonelli D (2021b). Seismic assessment and strengthening interventions of atop single-block rocking elements in monumental buildings: the case study of the San Felice sul Panaro Fortress. *SAHC 2020 - 12th International Conference on Structural Analysis of Historical Constructions*, Barcelona (Spain), 29-30 September – 1 October 2021.

Derakhshan H, Nakamura Y, Griffith MC, Ingham JM (2020). Suitability of Height Amplification Factors for Seismic Assessment of Existing Unreinforced Masonry Components. *Journal of Earthquake Engineering*, DOI: 10.1080/13632469.2020.1716889.

Di Domenico M, Ricci P, Verderame GM (2021). Floor spectra for bare and infilled reinforced concrete frames designed according to Eurocodes. *Earthquake Engng Struct Dyn.* 1-25, DOI: 10.1002/eqe.3523.

Dolce M, Nicoletti M, De Sortis A, Marchesini S, Spina D, Talanas F (2017). Osservatorio sismico delle strutture: the Italian structural seismic monitoring network. *Bulletin of Earthquake Engineering* 15(2): 621-641.

Eurocode 8. Design of Structures for Earthquake Resistance. Part 1-1: General Rules, Seismic Actions and Rules for Buildings. Brussels; 2004:229

Fathi A, Sadeghi A, Emami Azadi MR, Hoveidae N (2020). Assessing the soil-structure interaction effects by direct method on the out-of-plane behavior of masonry structures (case study: Arge-Tabriz). *Bull. Earthq. Eng.*18:6429-6443.

Hamidia M, Shokrollahi N, Nasrolahi M (2021). Soil-structure interaction effects on the seismic collapse capacity of steel moment-resisting frame buildings. *Structures*, 32:1331-1345.

Karapetrou ST, Fotopoulou SD, Pitilakis KD (2015). Seismic vulnerability assessment of high-rise non-ductile RC buildings considering soil-structure interaction effects. *Soil Dyn. Earthq. Eng.* 73:42-57.

Karatzetzou A, Pitilakis D, Kržan M, Bosiljkov V (2015). Soil-foundation-structure interaction and vulnerability assessment of the Neoclassical School in Rhodes, Greece. *Bull Earthq Eng.*,13:411-428.

Kazantzi AK, Vamvatsikos D, Miranda E. (2020a). Evaluation of Seismic Acceleration Demands on Building Nonstructural Elements. *J. Struct. Eng*.146(7): 04020118

Kazantzi AK, Vamvatsikos D, Miranda E. (2020b). The effect of damping on floor spectral accelerations as inferred from instrumented buildings. *Bulletin of Earthquake Engineering* 18:2149–2164.

Lagomarsino S, Penna A, Galasco A, Cattari S (2013). TREMURI program: an equivalent frame model for the nonlinear seismic analysis of masonry buildings. *Eng Struct.* 56:1787-1799.

Lorenzoni F, Casarin F, Modena C, Caldon M, Islami K, da Porto F (2013). Structural health monitoring of the Roman Arena of Verona, Italy. *J Civil Struct Health Monit* 3(4):227-246.

Lorenzoni F, Lazzarini L, Calabria A, de Conto N, da Porto F (2019). Assessment of the dynamic response of monitored masonry buildings after the Central Italy earthquake swarm in 2016. *7th ECCOMAS Thematic Conference on Computational Methods in Structural Dynamics and Earthquake Engineering,* Crete, Greece.

Lucchini A, Franchin P and Mollaioli F (2017). Uniform hazard floor acceleration spectra for linear structures. *Earthq.Eng.Struct.Dyn.* 46(7), 1121-1140.

Magenes G, Penna A, Senaldi IE, Rota M and Galasco A (2014). Shaking Table Test of a Strengthened Full-Scale Stone Masonry Building with Flexible Diaphragms. *International Journal of Architectural Heritage* 8:3, 349-375.

Martakis P, Reuland Y, Chatzi E (2022). Amplitude Dependency Effects in the Structural Identification of Historic Masonry Buildings. In: Pellegrino C., Faleschini F., Zanini M.A., Matos J.C., Casas J.R., Strauss A. (eds) Proceedings of the 1st Conference of the European Association on Quality Control of Bridges and Structures. EUROSTRUCT 2021. Lecture Notes in Civil Engineering, vol 200. Springer, Cham. https://doi.org/10.1007/978-3-030-91877-4_17.

Menon A and Magenes G (2011a). Definition of seismic input for out of plane response of masonry walls: I. Parametric study. *J Earthq Eng* 15(2): 165-194.

Menon A and Magenes G. (2011b). Definition of seismic input for out of plane response of masonry walls: II. Formulation. *J Earthq Eng* 15(2): 195-213.

Merino RJ, Perrone D, Filiatrault A (2019). Consistent floor response spectra for performance-based seismic design of non-structural elements. *Earthq Eng Struct Dyn.* 49(3):261-284.

Michel C, Guéguen P (2010). Time-frequency analysis of small frequency variations in civil engineering structures under weak and strong motions using a reassignment method. *Structural Health Monitoring* 9(2):159–171.

Muscolino G (1991). Dinamica di sistemi strutturali composti da due sottostrutture, Chapter contribution to the book "Problemi Strutturali nell'Ingegneria Sismica", Dario Flaccovio Editore, 255-302 (in Italian).

NZSEE. New Zealand Society for Earthquake Engineering (NZSEE), Structural Engineering Society New Zealand Inc. (SESOC), New Zealand Geotechnical Society Inc., Ministry of Business, Innovation and Employment, Earthquake Commission. The Seismic Assessment of Existing Buildings (the Guidelines), Part C—Detailed Seismic Assessment; 2017. http://www.eq-assess.org.nz/

Oz I, Senel SM, Palanci M, Kalkan A (2020). Effect of Soil-Structure Interaction on the Seismic Response of Existing Low and Mid-Rise RC Buildings. *Applied Sciences* 10(23):8357.

Petrone C, Magliulo G and Manfredi G (2015). Seismic demand on light acceleration-sensitive nonstructural components in European reinforced concrete buildings. *Earthq.Eng.Struct.Dyn.* 44: 1203-1217.

Rodriguez D, Perrone D, Filiatrault A, Brunesi E (2021). A probabilistic strong floor motion duration model for seismic performance assessment of non-structural building elements. *Earthquake Engng Struct Dyn.* 50:4161–4179.

Senaldi I, Magenes G, Penna A, Galasco A, Rota M (2014). The Effect of Stiffened Floor and Roof Diaphragms on the Experimental Seismic Response of a Full-Scale Unreinforced Stone Masonry Building, *Journal of Earthquake Engineering* 18(3):407-443, DOI: 10.1080/13632469.2013.876946.

Senaldi IE, Guerrini G, Comini P, Graziotti F, Penna A, Beyer K, Magenes G (2020). Experimental seismic performance of a half-scale stone masonry building aggregate. *Bulletin of Earthquake Engineering* 18(2):609–643.

Sivori D, Lepidi M, Cattari S. (2021). Structural identification of the dynamic behavior of floor diaphragms in existing buildings, *Smart Structures and Systems*, 27(2): 173-191.

Sullivan TJ, Calvi PM, Nascimbene R (2013). Towards improved floor spectra estimates for seismic design. *Earthquake Struct.* 4(1):109-132.

Spina D, Lamonaca B (1998). Strengthening assessment of building using ambient vibration tests. In: Proceedings of the 11th European Conference on Earthquake Engineering, Paris, France

Surana M, Pisode M, Singh Y, Lang DH (2018). Effect of URM infills on inelastic floor response of RC frame buildings. *Eng Struct.* 175:861-878.

Vukobratović V, Fajfar P (2016). A method for the direct estimation of floor acceleration spectra for elastic and inelastic MDOF structures. *Earthq Eng Struct Dynam.* 45:2495-2511.

Vukobratović V, Fajfar P (2017). Code-oriented floor acceleration spectra for building structures. *Bull Earthq Eng.* 15(7):3013-3026.